Spatially varying peatland initiation, Holocene development, carbon accumulation patterns and radiative forcing within a subarctic fen

Sanna R. Piilo*[a,b], Atte Korhola[a,b], Lauri Heiskanen[c], Juha-Pekka Tuovinen[c], Mika Aurela[c], Sari Juutinen[a,b], Hannu Marttila[d], Markus Saari[d], Eeva-Stiina Tuittila[e], Jukka Turunen[f], Minna M. Väliranta[a,b]

[a] ECRU, Ecosystems and Environment Research Programme, Department of Environmental Sciences, University of Helsinki, P.O. Box 65, 00014, Finland

[b] Helsinki Institute of Sustainability Science (HELSUS), Finland

[c] Finnish Meteorological Institute, Erik Palménin aukio 1, 00560, Helsinki, Finland

[d] Water, energy and Environmental Engineering Research Unit, University of Oulu, P.O. Box 4300, 90014, Finland

[e] School of Forest Sciences, University of Eastern Finland, P.O. Box 111, Joensuu, Finland

[f]Environmental Solutions, Peatland Use and Resource Economics, Geological Survey of Finland, P.O. Box 96, 02151, Espoo, Finland

*Corresponding author: email: sanna.piilo@helsinki.fi

Abstract

High latitude peatlands act as globally important carbon (C) sinks and are in constant interaction with the atmosphere. Their C storage is formed during the Holocene. In the course of time, the aggregate effect of the C fluxes on radiative forcing (RF) typically changes from warming to cooling, but the timing of this shift varies among different peatlands. Here we investigated Holocene peatland development, including vegetation history, vertical peat growth and the lateral expansion of a patterned subarctic fen in northern Finland by means of multiple sampling points. We modelled the Holocene RF by combining knowledge on past vegetation communities based on plant macrofossil stratigraphies and present *in situ* C flux measurements. The peatland initiated at ca. 9500 calibrated years Before Present (cal. BP), and its lateral expansion was greatest between ca. 9000 and 7000 cal. BP. After the early expansion, vertical peat growth proceeded very differently in different parts of the peatland, regulated by internal and external factors. The pronounced surface microtopography, with high strings and wet flarks, started to form only after ca. 1000 cal. BP. C accumulation

rates varied spatially markedly throughout the peatland history, also during the recent past. We applied two flux scenarios with different interpretation of the initial peatland development phases to estimate the RF induced by C fluxes of the fen. After ca. 4000 cal. BP, at the latest, the peatland RF has been negative (cooling), mainly driven by C uptake and biomass production, while methane emissions had a lesser role in the total RF. Interestingly, these scenarios suggest that the greatest cooling effect took place around ca. 1000 cal. BP, after which the surface microtopography established. The study demonstrated that despite the high spatial heterogeneity and idiosyncratic behaviour of the peatland, the RF of the studied fen followed the general development pattern of more southern peatlands. The Holocene climate variations and warm phases did not seem to induce any distinctive and consistent peatland-scale patterns in C accumulation, whereas our data suggests that the changes in vegetation related to the autogenic succession were reflected in the C accumulation patterns and RF more clearly.

Keywords: subarctic fen, peatland, radiative forcing, carbon accumulation, Holocene, lateral expansion, paleoecology, vegetation dynamics

1. Introduction

Northern peatlands are an important element in the global carbon (C) cycle and act as a C sink, representing ca. 90% of the 545 (475–620) Gt C stored in peatlands globally (Yu et al., 2010), the estimates of C sink ranging up to 1055 Gt C (Nichols and Peteet, 2019). Northern peatlands are globally essential C stores with ca. one third of all soil C stored in them due to the slow decomposition in waterlogged conditions and low temperatures (Gorham, 1991). Due to the changing climate, the C storage accumulated during the Holocene may be compromised. High latitudes are warming at a rate twice the global average (IPCC, 2013), and the Arctic has already warmed by 2–3°C since the late 19th century (Post et al., 2019) and precipitation has increased by 6 % during the past ca. 50 years (Box et al., 2019). High uncertainties are especially related to future precipitation (Box et al., 2019; Collins et al., 2013), which will together with the temperature rise, affect peatland moisture conditions and thus vegetation assemblages and C accumulation capacity especially in northern regions (McGuire et al., 2018; Helbig et al., 2020).

Post-glacial peatland initiation in high latitudes overall was triggered by rising growing season temperatures and the availability of excess water (Morris et al., 2018) and peaking in the early Holocene 11,000–9000 calibrated years before present (cal. BP; present = 1950 Anno Domini) (MacDonald et al., 2006; Ruppel et al., 2013; Yu et al., 2010). As interpreted from peat archives, Holocene climate variations are reflected in peatland dynamics (Charman et al., 2013; Yu et al., 2009). For example, during the warm Medieval Climate Anomaly (MCA; 1000–700 cal. BP (Mann et al., 2009)) and Holocene thermal maximum (HTM; 8000–4800 cal. BP (Renssen et al., 2012)), increased net primary productivity (NPP) exceeded peat decomposition, leading to accelerated peat accumulation (Charman et al., 2013; Yu et al., 2009). In contrast, over the climate transition from the MCA to the Little Ice Age (LIA; 500–100 cal. BP (Wilson et al., 2016)), C sequestration rate of northern peatlands declined, possibly because of the lower temperatures combined with increased cloudiness, which suppressed NPP (Charman et al., 2013).

Peatlands exchange greenhouse gases (GHG) with the atmosphere, which generates radiative forcing (RF) with climatic implications. A negative (cooling) RF results from net uptake of carbon dioxide (CO_2), while the methane (CH_4) emissions have an opposite (warming) impact associated with positive RF (Frolking and Roulet, 2007; Yu, 2011). In general, peatlands simultaneously sequester and release C, the balance associated with the peatland surface microtopography (Alm et al., 1999; Waddington and Roulet, 2000). During its succession, a peatland may act as both a C sink and a source, depending on various simultaneously affecting autogenic and allogenic forcing factors (Korhola et al., 1996; Yu, 2011). While the net RF depends on the balance between CO_2 and CH_4 fluxes, it is important to note that these two gases differ greatly in their radiation efficiency and residence time in the atmosphere (Myhre et al., 2013). Therefore, the initial net

67 RF effect of a newly developed peatland is mainly warming, due to the dominance of CH_4 emissions. Over the course of
68 time, however, the negative RF due to sustained CO_2 sequestration exceeds the CH_4 –induced positive forcing, which
69 leads to a negative net RF, i.e. cooling effect (Frolking and Roulet, 2007; Mathijssen et al., 2014).

70 The Holocene C dynamics of subarctic permafrost-free fens have received less attention (Juutinen et al., 2013; Mäkilä et
71 al., 2001; Mäkilä and Moisanen, 2007; Mathijssen et al., 2014) than C dynamics of permafrost peatlands (e.g. Gałka et
72 al., 2018; Pelletier et al., 2017; Sannel et al., 2017; Zhang et al., 2018a) or boreal bogs (e.g. Korhola et al., 1996;
73 Mathijssen et al., 2016; Turunen et al., 2001; Van Bellen et al., 2011). Fens, however, respond to changes in the
74 environment, especially moisture conditions, more strongly and faster than bogs (Gong et al., 2013; Jaatinen et al., 2007;
75 Kokkonen et al., 2019; Tahvanainen, 2011; Wu and Roulet, 2014). Moreover, a pronounced decline in C accumulation
76 over the warm and dry mid-Holocene climate phase (ca. 8000–5000 cal. BP (e.g. Eronen et al., 1999; Seppä et al., 2009))
77 has been recorded for subarctic fens (Mäkilä and Moisanen, 2007; Mathijssen et al., 2014; Robinson, 2006). This
78 contradicts the patterns reported by Yu et al. (2009) for northern peatlands, where an overall slowdown of C accumulation
79 after 4000 cal. BP was connected to climate cooling following the high accumulation rates over the warm mid Holocene.
80 As motivated by the current highly pronounced warming in the subarctic region, there is a need to deepen our
81 understanding of the connections between climate and the ecosystem processes, C dynamics and atmospheric forcing of
82 subarctic fens.

83 Here, we aim to link the long-term history of a subarctic Kaamanen peatland to its present-day C dynamics. To contribute
84 to the understanding of the future peatland-climate interactions and scenarios, we explored how the Holocene warm
85 climate phases, i.e. HTM, MCA and recent warming since the 1980s, are reflected in peatland physical and biological
86 dynamics and what was the consequent radiative forcing effect. To reconstruct C flux dynamics since the peatland
87 initiation by combining palaeoecological data with contemporary measurements, we take advantage of the present-day
88 GHG flux measurements conducted at the site and within its catchment. At the site, the ecosystem-atmosphere exchange
89 of CO_2 has been measured using eddy covariance (EC) technique since 1997 (Aurela et al., 2004, 2002, 2001, 1998), and
90 plant community specific GHG fluxes have been measured by chambers (Maanavilja et al., 2011; Heiskanen et al. 2020).
91 Under the current climate conditions, the peatland is a weak C sink of ca. -20 g C m^{-2} yr^{-1} on average (Aurela et al., 2004;
92 Hargreaves et al., 2001; Heiskanen et al. 2020). Reconstruction of the peatland development history, initiation and
93 subsequent lateral expansion, allowed us to use these flux data to model the RF of the fen from its initiation to the present.

94 **2. Material and methods**

95 *2.1 Site description*

Our study peatland (Kaamanen, 69° 8.44′ N, 27° 16.19′ E, 155 m a.s.l.) is a subarctic patterned flark fen (ca. 43 ha) characteristic of the northern aapa mire region (Figure 1). The long-term (1981–2010) mean annual air temperature and precipitation sum are -0.4°C and 472 mm, respectively (Pirinen et al., 2012). Direction of water flow is from north to south, and spring flooding is typical. Strings (hummocks) and flarks (hollows) with a dimension of few metres create a patterned mosaic of surface microtopography. Ombrotrophic strings are typically lower than 1 m, but extend clearly above the surrounding water table, and can remain frozen inside until late summer (Maanavilja et al., 2011). The Kaamanen peatland is located within the sporadic permafrost zone, the so-called palsa mire zone (Figure 1), but has no permafrost. The inundated flarks close to a small stream, lining the east of the studied fen area, are mesotrophic. The prevailing vegetation varies greatly among different parts and microtopographic features of the fen. Flark vegetation is mainly composed of sedges *Carex spp., Trichophorum cespitosum* and *Eriophorum angustifolium,* a forb *Menyanthes trifoliata* and brown mosses (typically *Scorpidium scorpioides*). Tall sedge vegetation fringes the stream. Strings are dominated by forest and hummock mosses such as *Dicranum spp.* and *Pleurozium schreberi,* lichens, and dwarf shrubs *Rhododendron tomentosum, Empetrum nigrum, Vaccinium uliginosum, V. vitis-idaea* and *Rubus chamaemorus.* Dwarf shrubs *Andromeda polifolia, Betula nana* and *Salix spp.* and peat mosses *Sphagnum fuscum* and *S. capillifolium* are found at the margins of the strings (Maanavilja et al. 2011). Wet lawns with *S. lindbergii* and low hummocks characterised by *S. fuscum* and dwarf shrubs dominate the south-west part of the study area. *Pinus sylvestris* forest and small lakes surround the peatland. Peat thickness in the northern part of the fen is ca. 1 m, but in the south, closer to the lake, it is up to 4 m (Figure 1).

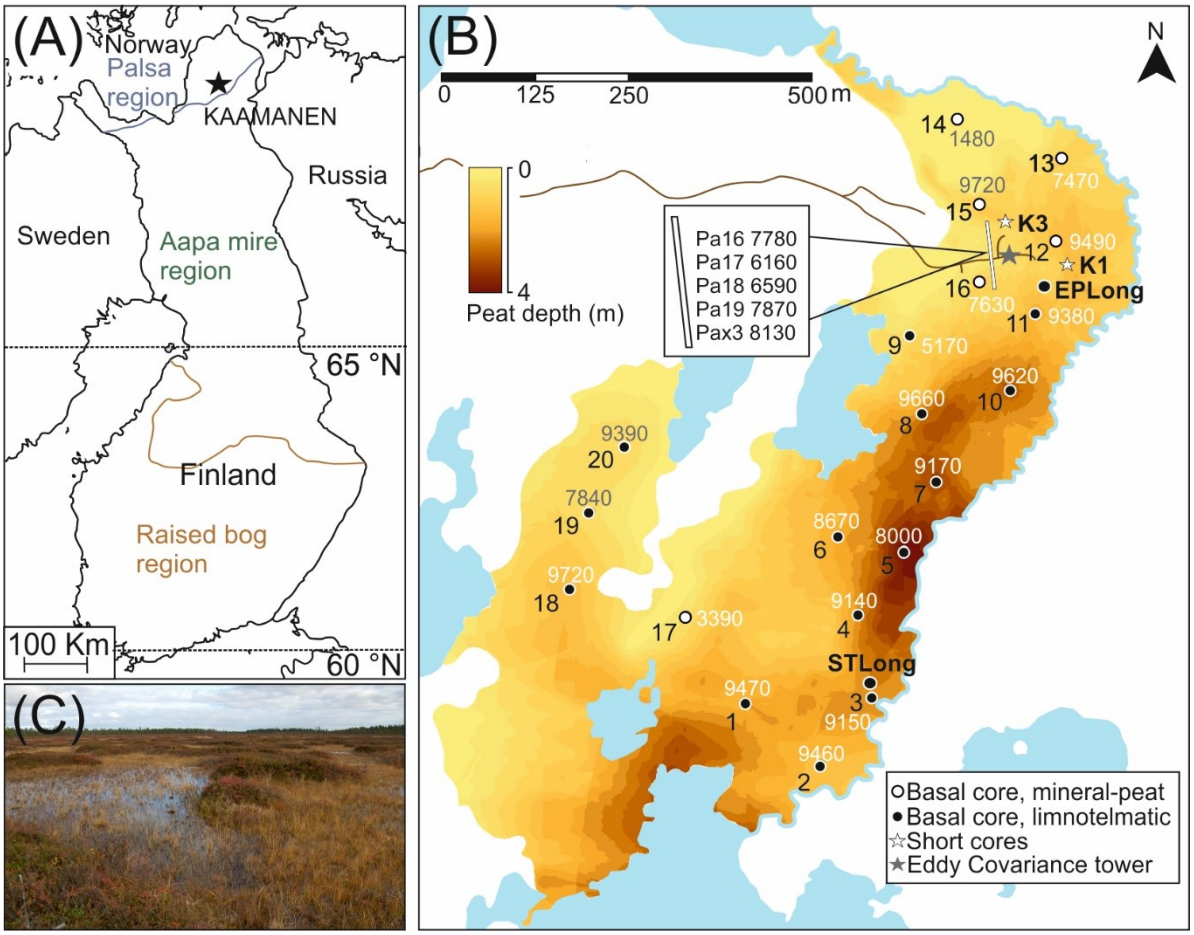

Figure 1. Study area located in northern Finland (A). The black star shows the location of the study site and the coloured lines indicate the distribution of raised bogs (ombrotrophic peatlands), aapa mires (peatland complexes with minerotrophic fen conditions in the central parts) and palsa peatlands (fens with frozen peat mounds) in Finland. (B) Isochrone map of the studied peatland area and the peat thickness. Coring locations are shown with dots and white stars with the number or the name of the location and calibrated basal ages (cal. BP). White line with Pa –codes indicates a coring transect. (C) The microtopographic variation of flarks and strings.

2.2 Peat thickness measurement and sampling

We selected the coring locations based on a ground-penetrating radar (GPR, Malå GeoScience ProEx) survey of the peat thickness and the underlying topography, conducted during the snow cover period in April 2018. The total length of measurement transects was 9.6 km which were measured using a snowmobile to pull the antennae (50 MHz, approximate velocity 5 m s^{-1}). The measurement transects and the data analysis were performed using the ReflexW (Version 8.0, Sandmeier, 2016) programme. Measured subsoil, peat and sediment thickness data were used as validation of the radar data.

To address initial and long-term development, twenty basal peat samples, representing the first peat on a top of the minerogenic sediment were collected with a Russian peat corer (3 x 50 cm). A long core from *Sphagnum-Trichophorum* surface (STLong 393 cm) was collected in September 2018 and one long core from Ericales-*Pleurozium* surface in the string top (EPLong 228 cm) in 2010 (Figure 1). An additional short transect of basal samples was collected in 2009 from the northern part of the peatland (Figure 1). To address more recent development additional four short cores were collected with a box corer (7 x 4 x 65 cm) in September 2016. To cover the spatial variability, the short cores were collected from string margins with *Betula-Sphagnum* vegetation (K1BS, K3BS) and from the dry strings (K1EP, K3EP) with Ericales-*Pleurozium* vegetation. Short cores were collected from the northern part of the peatland, where surface microtopography is more pronounced. Cores were wrapped in plastic and transported, avoiding compaction, inside plastic tubes to the University of Helsinki. Cores were cut to 1 or 2 cm slices and the subsamples were stored in plastic bags at 6 °C.

2.3 Plant macrofossil analysis

Plant macrofossil analysis was conducted to detect and to reconstruct changes in vegetation assemblages. In the short cores, the analysis was performed at 2 cm resolution and in the EPLong long core at every 10 cm and in STLong core at every 20 cm. Volumetric samples (5 ml) were inspected following Mauquoy and van Geel (2007) as modified by Väliranta et al. (2007). Samples were rinsed with water using a 140-µm sieve and the residue was analysed for proportions of main peat components. A stereomicroscope was used for estimating percentages of a total sample volume and a light microscope for further species level identification (for identification: e.g. Laine J. et al. 2009; Eurola et al. 1992 and a reference collection at the University of Helsinki). Seeds and leaves were counted as exact numbers (Figure A.1). Percentage of unidentified organic material (UOM) was estimated if the organic remains were unidentifiable for the vegetation type. Diagrams were created using software C2 (Juggins, 2007) and Tilia 2.0.41 (Grimm, 1991).

2.4 Chronology

A total of 33 samples were sent for accelerator mass spectrometry (AMS) ^{14}C analysis to Poznan Radiocarbon Laboratory (Poznan, Poland), 19 samples to the Finnish Museum of Natural History (LUOMUS, Helsinki, Finland) and 3 samples were dated in A. E. Lalonde AMS Laboratory (University of Ottawa) (Tables A.1 and B.1). Either bulk peat, cleaned from rootlets (Holmquist et al., 2016), or identified plant macrofossils were selected for dating (Table B.1). Basal samples were ^{14}C dated to reconstruct the lateral expansion of the peatland following the procedure introduced in Korhola (1994). To depict changes in vegetation type, two long cores and four short surface cores were ^{14}C dated. The two long cores taken from a wet *Sphagnum – Trichophorum* flark (STLong) and dry Ericales – *Pleurozium* string (EPLong) were dated only by ^{14}C. For both long cores, basal ages from the nearest basal peat sampling points were used

157 instead of the original bottom-most ages of the cores, because the obtained ages show inconsistencies with different
158 materials dated. Dated *Equisetum* remains provided consistently younger ages than selected terrestrial plant
159 macrofossils (*Carex* spp. seeds, *Betula* seeds, *Potentilla palustris* seeds, *Salix* sp., bark and woody remains) (Table B.1)
160 (Howard et al., 2009; Väliranta et al., 2014). For the STLong, the bottom-most age was from a basal peat sample from
161 the nearest coring point 3 and for EPLong from coring point 11 (Figure 1).
162 The four surface cores were additionally ^{210}Pb dated at the University of Exeter, UK, using alpha-spectrometry at 2 cm
163 intervals. 0.2−0.5 g of dried and ground peat from each depth were analysed and spiked with a ^{209}Po yield tracer (Kelly
164 et al., 2017; Estop-Aragonés et al., 2018 for the method). Constant Rate of Supply model (CRS) was applied to obtain
165 the ^{210}Pb ages (Appleby and Oldfield, 1978). Age-depth models (Figure 2), combining both the ^{14}C results and ^{210}Pb
166 dates were created with BACON v2.3.3 package (Blaauw, 2010; Blaauw and Christen, 2011) in R version 3.4.3 (R
167 Development Core Team 2016).

168 *2.5 Peat properties and C accumulation*

169 To determine dry bulk density (g cm^{-3}) of subsamples, we measured dry mass (g) of peat fresh volume of 5 cm^3. For the
170 short cores, C and nitrogen (N) content at 4 cm intervals was measured using a LECO TruSpec micro Elemental
171 Determinator, at the University of Helsinki, and these results were applied to calculate average values for the layers
172 between the measurements. For the two long cores, loss on ignition (LOI) was measured at 10 cm intervals, following
173 Heiri et al. (2001) and C content was estimated assuming 50% of C in organic matter (LOI x 0,5) (Loisel et al., 2014).
174 Apparent C accumulation rates (CAR, g C m^{-2} yr^{-1}) were calculated by multiplying the C mass of each 1 cm increment
175 (g m^{-3}) by the corresponding peat growth rate (m yr^{-1}) (Tolonen and Turunen, 1996), derived from the age-depth models
176 (Figure 2).

177 *2.6 Annual CO_2 and CH_4 balances*

178 In order to model the RF due to peatland development at Kaamanen, we estimated the ecosystem-atmosphere exchange
179 of CO_2 and CH_4 for different vegetation assemblages based on present-day flux measurements. These assemblages were
180 classified as aquatic ('Sandy *Equisetum'*), *Equisetum*-dominated fen communities ('Peaty *Equisetum',* i.e. on organic
181 sediments), non-patterned fens and their composites, which occurred during different development phases before the
182 present patterned fen phase. We reconstructed the successional development areas (QGIS 3.0.0) for these different
183 paleovegetation types by applying dating results and the reconstructed vegetation history. The flux measurements were
184 made both with the eddy covariance (EC) and chamber techniques, the former providing areally averaged and the latter
185 plant-community-specific data. Mean annual fluxes (Table 1) were obtained by accumulating the measurement data by

means of empirical response models driven by environmental variables, such as temperature and irradiance, and by linear interpolation (Aurela et al., 2002; Juutinen et al., 2013; Laine A. et al., 2009; Heiskanen et al. 2020).

Table 1. Flux densities (g C m^{-2} yr^{-1}) adopted for different peatland vegetation assemblages and used for the radiative forcing modelling. Values for "non-patterned fen" are obtained from *Trichophorum* and of *Carex-Scorpidium* dominated surface measurements. "Patterned fen" represents the current peatland spatially averaged estimate based on the EC data. * Values from Juutinen et al. (2013).

	Flux density (g C m^{-2} yr^{-1})		
	CO_2	CH_4	CO_2+CH_4
Sandy *Equisetum**	-10	-0.4	-10
Peaty *Equisetum**	18	5	23
Mix of non-patterned fen & Peaty *Equisetum*	-15	7	-8
Non-patterned fen	-48	8	-39
Patterned fen	-18	6	-12

The EC data (Aurela et al., 2004; Heiskanen et al., 2020) were used for the current phase, i.e. the past 1000 yr, when the peatland has exhibited pronounced microtopographical heterogeneity and been dominated by four vegetation habitats: (1) *Trichophorum* tussock flarks, (2) wet *Carex-Scorpidium* flarks, (3) *Sphagnum-Betula nana* string margins and (4) Ericales-*Pleurozium* string tops, defined in Maanavilja et al. (2011). The areal coverage of these habitats was determined by drone imaging with very high spatial resolution within a 200-m radius from the EC measurement tower (Räsänen et al., 2019). The EC data cover eight years for both CO_2 (1997–2002, 2017–2018) and CH_4 (2011–2018) fluxes.

Both EC measurements and flux chamber data of the *Trichophorum* and *Carex-Scorpidium* communities were used to reconstruct the past C exchange of the Cyperaceous fen during a phase when the present microtopographical features were not yet developed (Heiskanen et al., 2020). During the growing season, the relative difference between the EC- and chamber-based data was used to scale the chamber-based CO_2 fluxes to match the EC fluxes separately for the ecosystem respiration and gross primary production estimated from the data (Aurela et al., 2002; Heiskanen et al., 2020). Outside the growing season, the EC-based CO_2 fluxes were allocated proportionally to the *Trichophorum* and *Carex-Scorpidium* communities based on the respiration fluxes measured with chambers during the last two weeks of

207 the growing season. The annual CH_4 balance was partitioned to these plant communities similarly to the CO_2 balance by
208 partitioning the EC data according to the scaled chamber-based plant-community-specific fluxes. An equal coverage of
209 *Trichophorum* and *Carex-Scorpidium* communities was assumed for the flux reconstruction.

210 In addition to the local fluxes, we included flux data measured with chambers (year around estimate complemented by
211 snow-gradient measurements) across the Kiposuo peatland – Kipojärvi lake continuum, located within the same
212 catchment ca. 6 km northeast of Kaamanen (Laine A. et al., 2009; Juutinen et al., 2013). These data represent aquatic
213 vegetation communities in shallow water conditions (*Equisetum fluviatile*, mixed *E. fluviatile* and *Carex* spp.) and were
214 here adopted for an early *Equisetum*-limnotelmatic phase of the study peatland. Two different vegetation types were
215 included: (1) littoral vegetation patches on sandy sediments ('Sandy *Equisetum*'), with net uptake of C, and (2) littoral
216 vegetation on organic sediments ('Peaty *Equisetum*'), with net release of C.

217 These two data sets make it possible to assess how the likely release of excess CO_2 from the peatland-lake ecotone to
218 the atmosphere affects the RF simulation. In other words, we assumed that the current peatland, at places where it
219 developed from a limnic system, has been a temporary net C source due to release of CO_2 from the net heterotrophic
220 littoral zone.

221 Two alternative simulation scenarios were outlined for the *Equisetum* fluxes. In Scenario 1, we used the flux
222 measurements from the 'Sandy *Equisetum*' habitat for the earliest phase of the peatland, since underneath the paleo-
223 vegetation layer lies mineral ground and thus this paleo-habitat resembles littoral sand conditions. For the peatland
224 development phases following this, we adopted 'Peaty *Equisetum*' as the representative habitat. In Scenario 2, we used
225 the fluxes from littoral sand for the first 1000 yr and linearly interpolated between them and the fluxes of 'Peaty
226 *Equisetum*' for the following four millennia, assuming that this represents the change from littoral conditions to peat-
227 forming vegetation. For the vegetation assemblage 'Mix of non-patterned fen and Peaty *Equisetum*', inferred from the
228 plant macrofossil analysis, we used the average of the corresponding fluxes.

229 ### 2.7 *Radiative forcing modelling*

230 The areas of different vegetation assemblages were multiplied by the corresponding flux densities (g m^{-2} yr^{-1}) (Table 1)
231 to obtain the total CO_2 and CH_4 fluxes (g yr^{-1}) for the Kaamanen peatland during each 1000-yr slot from 10,000 cal. BP
232 to the present. Changes to Earth's radiative balance, i.e. radiative forcing, due to perturbations in atmospheric
233 concentrations induced by these fluxes was calculated in annual steps with the sustained impulse-response model
234 described by Lohila et al. (2010) and Mathijssen et al. (2017). The decaying perturbation to the atmospheric CO_2 storage
235 is modelled as a weighted sum of four exponential functions that represent different time scales involved in the global

biogeochemical CO_2 cycles. The longest time scale effectively corresponds to a permanent effect for 22% of the concentration change. The corresponding model for CH_4 assumes a first-order decay with a perturbation time scale of 12.4 yr. Since Mathijssen et al. (2017), the RF model has been updated to include the indirect RF due to atmospheric CH_4-to-CO_2 oxidation (Boucher et al., 2009), revised radiative efficiencies (Etminan et al., 2016) and the variations in atmospheric mixing ratios of CO_2, CH_4 and nitrous oxide (Köhler et al., 2017).

3. Results

3.1 Age-depth models and peat growth rates

Peat growth rate in EPLong (Ericales – *Pleurozium* string), was, on average, 0.2 mm yr^{-1} from ca. 9270 cal. BP (227 cm) to ca. 95 cal. BP (43 cm). The average and the highest peat growth rates in STLong (*Sphagnum* – *Trichophorum* flark) were 0.4 and 0.6 mm yr^{-1} (between ca. 8330 cal. BP (325 cm) and 6070 cal. BP (190 cm)), respectively (Figures 2 and 3).

Based on the established age-depth models using ^{14}C and ^{210}Pb dating results, peat growth rates had not been constant during the shorter time scale either (Figures 2 and 4). For K1EP, the peat growth rate was fast between ca. 1290 (58 cm) and ca. 1050 (30 cm) cal. BP, on average 1.2 mm yr^{-1}. Between ca. 1050 and ca. 120 cal. BP, peat growth rates slowed down to an average of 0.2 mm yr^{-1} and then fastened to 1.1 mm yr^{-1} lasting until present (figure 2). For K1BS, average peat growth rate was first 0.5 mm yr^{-1} (from ca. 1980 (57 cm) to 1420 (30 cm) cal. BP) and then decreased to an average of 0.09 mm yr^{-1} (until ca 270 cal. BP (20 cm)). Towards the surface, the average peat growth rate increases to 0.7 mm yr^{-1} (ca. -60 cal. BP (5 cm)) and for the top-most layers it reached 6 mm yr^{-1}.

For K3 short cores, peat growth rates were more consistent over time than in K1 short cores and showed two distinct phases of low and higher rates (Figures 2 and 4). For K3EP, low average peat growth rate of 0.2 mm yr^{-1} was detected between ca. 1270 (59 cm) and ca. 450 (40 cm) cal. BP, after which the peat growth rate increased to 0.8 mm yr^{-1} lasting until the present. For K3BS, the low average peat growth rate phase of 0.1 mm yr^{-1} started from ca. 2690 cal. BP (57 cm) and lasted until ca. 370 cal. BP (35 cm), followed by an average peat growth rate of 1.6 mm yr^{-1} with higher rates in the top-most layers.

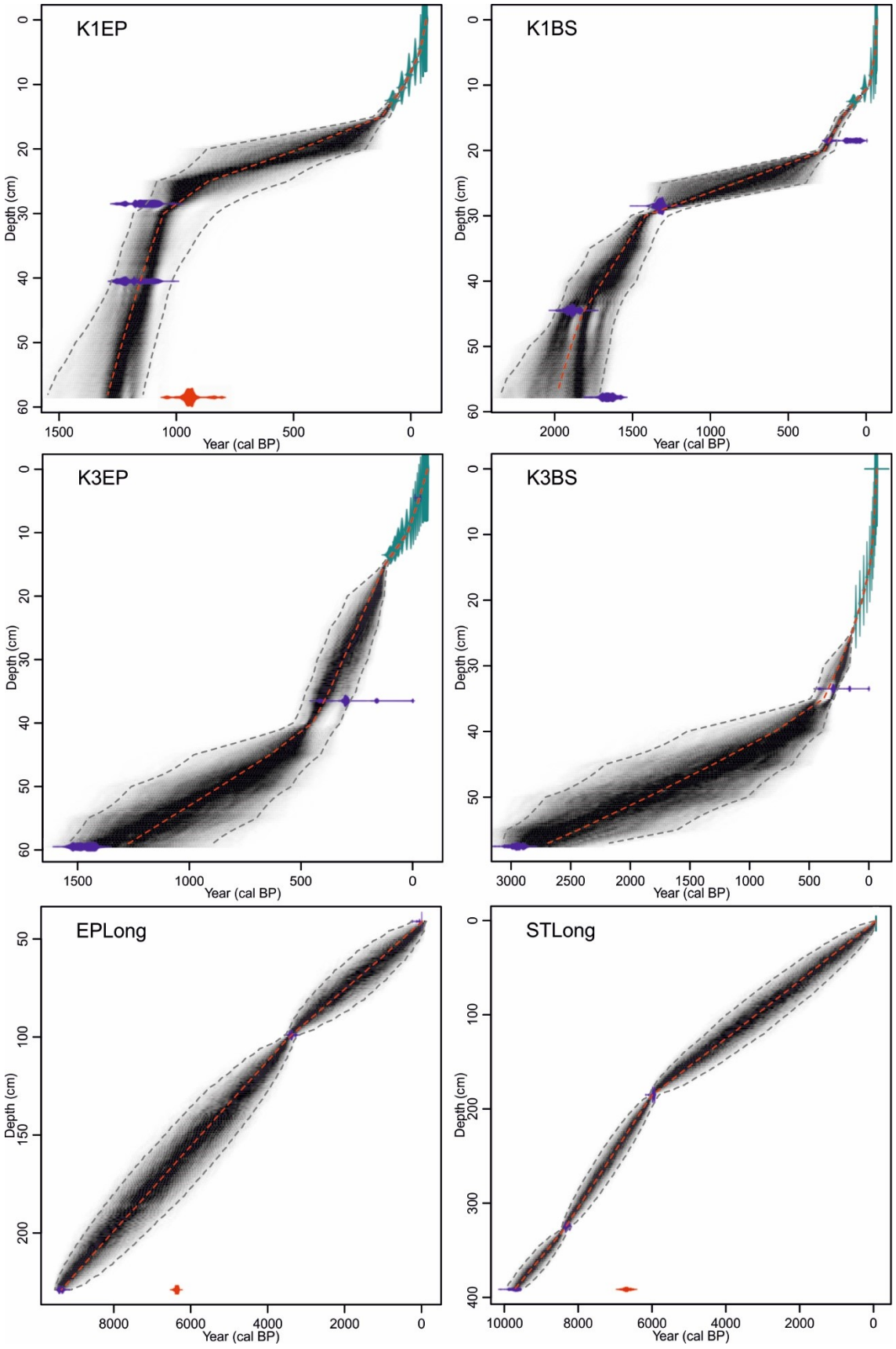

Figure 2. BACON derived age-depth models. In green: ^{210}Pb age-ranges (for K1 and K3 cores), and in violet: ^{14}C dates (cal. BP). The grey shading with the darkest grey demarks most likely age-range and the thin red line shows the weighted

mean age based on the model. In red are ^{14}C outliers (K1EP, EPLong and STLong). Notice the differences in the x and y-axis scales.

3.2 Plant community changes and peat properties

STLong: The early assemblages dated to ca. 9500 cal. BP contained remains of aquatic taxa such as *Charophyta* oospores and *Nymphaeaceae* together with wet indicating bryophytes. After the initial aquatic state, *Equisetum* and Cyperaceae with some woody remains dominated the plant community (Figure 3, Figure A1). *Menyanthes trifoliata*, *Potentilla palustris* and *Potamogeton* seeds were detected at ca. 8650 cal. BP (340 cm) with some *Sphagnum teres*. Between ca. 9640 to 6360 cal. BP (388–207.5 cm) the organic content (LOI) varied between 40% and 74%. Between ca. 6230 and 3850 cal. BP (200–120 cm) vegetation was a mixture of *Equisetum* and Cyperaceae. From ca. 6200 cal. BP (197.5 cm), organic content sharply increased with a marked decrease in peat dry bulk density. Organic content varied between 86% and 97% characteristic for sedge-dominated peat to the top of the core with a decrease in dry bulk density towards the surface (Figure 3). After ca. 4490 cal. BP, vegetation changed towards proper fen vegetation mainly composed of Cyperaceae such as *Carex* spp. *Eriophorum* sp. prevailing between ca. 1220 and 570 cal. BP (40 cm and 20 cm). Sedges and *Sphagnum warnstorfii* dominated the surface. Average dry bulk density was 0.14 g cm^{-3}.

EPLong: The assemblage was first dominated by *Equisetum* remains with some Cyperaceae and woody remains (Figure 3, Figure A.1), also mineral material was abundant. LOI first fluctuated between ca. 9270 and 8000 cal. BP with values ranging from 43% (199 cm) to 85% (209 cm) (Figure 3). After ca. 8000 cal. BP (199 cm), LOI values stayed high between 74% and 95%, typical for fen peat. Between ca. 8960- 6200 cal. BP (220–160 cm) *Menyanthes trifoliata* and *Potentilla palustris* seeds were present. *Carex* spp. seeds and *Betula nana* remains were abundant from ca. 7580 to 3430 cal. BP (190–100 cm). Roughly, after 7070 cal. BP (179 cm), vegetation composition became dominated by Cyperaceae with occasional *Sphagna* and other bryophytes. *Equisetum* remains disappeared after ca. 3380 cal. BP (99 cm). *Eriophorum vaginatum* remains appeared around 3430 cal. BP and were present until ca. 1060 cal. BP (100–60 cm). *Sphagnum fuscum* and *S. warnstorfii* dominated the top part, which was not inspected in further detail, from 40 cm (ca. -20 cal. BP). Relatively even dry bulk density values were observed throughout the core with an average of 0.17 g cm^{-3}. Dry bulk density slightly decreased towards the surfaces of the core, i.e. during the last ca. 150 years

K1EP and K3EP (string top sections): Both sites experienced a change from wetter fen vegetation to dry string conditions: K1EP at ca. 1020 cal. BP and K3EP at ca. 430 cal. BP (Figure 4, Figure A.1), i.e. there was a 600-years difference between the two close-by sites. In K1EP, the plant assemblage of the wet fen phase was highly humified (high proportion of UOM) Cyperaceae peat with *Eriophorum* starting from ca. 1290 cal. BP (58 cm). After ca. 1020 cal. BP (29 cm), plant composition changed to dwarf shrub roots, bark and leaves. At ca. 90 cal. BP (13 cm), *Hylocomium*

splendens and *Dicranum fuscenscens* emerged. In the top-most 5 cm, *Empetrum nigrum* leaves were abundant. The wet fen section of the K3EP was also dominated by Cyperaceae (from ca. 1270 cal. BP, 59 cm) with *Betula* periderm. The plant assemblages changed through a *Betula-Sphagnum* string margin type (ca. 430 cal. BP, 39 cm) into Ericales-*Pleurozium* string top vegetation (ca. 290 cal. BP, 28 cm) with dwarf shrub roots and *Hylocomium splendens* and *Pleurozium schreberi*. *Betula nana* and Ericales leaves and bud scales were abundant from the *Betula-Sphagnum* string margin phase throughout the string vegetation development. Average dry bulk density for both string top sections was 0.16 g cm^{-3}. Bulk densities decreased towards the surface taking place between ca. 400 and 100 cal. BP. The centennial-scale declining trend was less pronounced in the string top K1EP, where a decrease occurred only during the recent decades (Figure 4).

K1BS and K3BS (string margin sections): String margins showed unanimous changes in plant assemblages. K1BS core was first (ca. 1980 cal. BP, 57 cm) dominated by Cyperaceae with *Eriophorum vaginatum* and *Carex.* From ca. 1820 cal. BP (45 cm) to ca. 1190 cal. BP (28 cm) *Sphagnum* section Acutifolia dominated and *Andromeda polifolia* seeds were found (Figure 4, Figure A.1). *Eriophorum vaginatum* was dominating ca. one-hundred year period (28–27 cm) and *Empetrum nigrum* leaves were present. *Sphagnum fuscum* dominated between ca. 380 and 90 cal. BP (21–13 cm). Species composition typical to string top vegetation i.e., dwarf shrub roots, *Dicranum* sp. and *Pleurozium shreberi* were abundant between ca. 50 and -60 cal. BP (12–5 cm), after which plant assemblages returned to *S. fuscum* domination until the surface of the core. K3BS was at first dominated by Cyperaceae (*Carex* spp. and *Eriophorum vaginatum*) and *Scorpidium scorpioides* from ca. 2690 (57 cm) until ca. 380 cal. BP (35 cm). At ca. 350 cal. BP (34 cm), plant assemblage changed and was dominated by *S. fuscum* and *S. capillifolium*, but towards the surface was solely *S. fuscum* dominated. Dwarf shrub roots and leaves were also found. Average dry bulk density for both string margin sections was 0.11 g cm^{-3}. Bulk densities decreased towards the surface taking place between ca. 600 and 450 cal. BP.

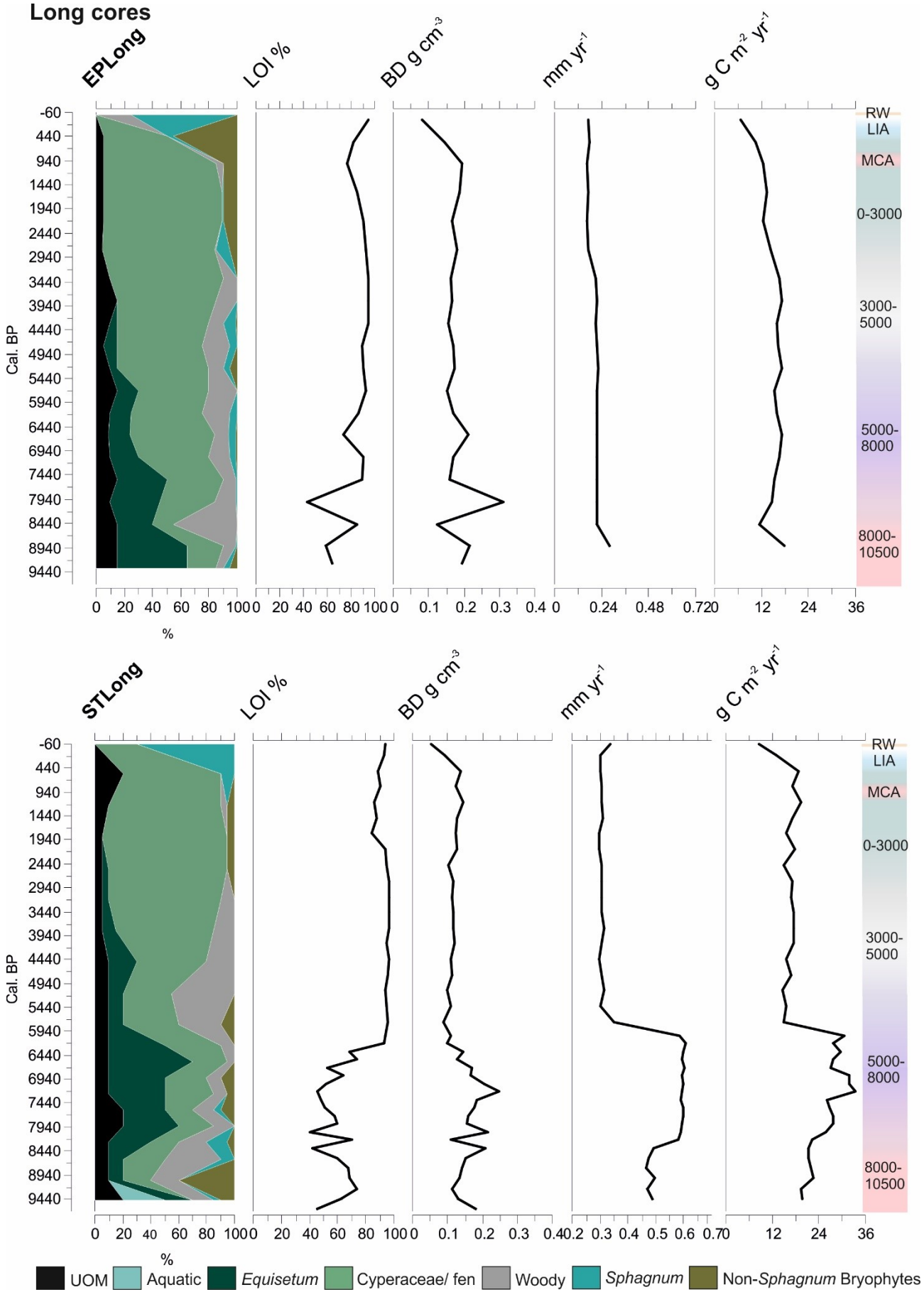
Long cores
EPLong
LOI %
BD g cm-3
mm yr-1
g C m-2 yr-1
Cal. BP
-60
440
940
1440
1940
2440
2940
3440
3940
4440
4940
5440
5940
6440
6940
7440
7940
8440
8940
9440
RW
LIA
MCA
0-3000
3000-5000
5000-8000
8000-10500
0 20 40 60 80 100
0 20 40 60 80 100
0 0.1 0.2 0.3 0.4
0 0.24 0.48 0.72
0 12 24 36
%
STLong
LOI %
BD g cm-3
mm yr-1
g C m-2 yr-1
Cal. BP
0 20 40 60 80 100
0 20 40 60 80 100
0 0.1 0.2 0.3 0.4
0.2 0.3 0.4 0.5 0.6 0.7
0 12 24 36
%
UOM
Aquatic
Equisetum
Cyperaceae/ fen
Woody
Sphagnum
Non-Sphagnum Bryophytes

313

Figure 3. Abundance of selected vegetation assemblages (%). Organic content as loss on ignition (LOI%), dry bulk density (BD g cm^{-3}), peat growth rate (mm yr^{-1}), apparent C accumulation rate (g C m^{-2} yr^{-1}). Climate phases (approximate cal. BP), Recent warming (RW), Little Ice Age (LIA) and Medieval Climate Anomaly (MCA) are indicated with different colours.

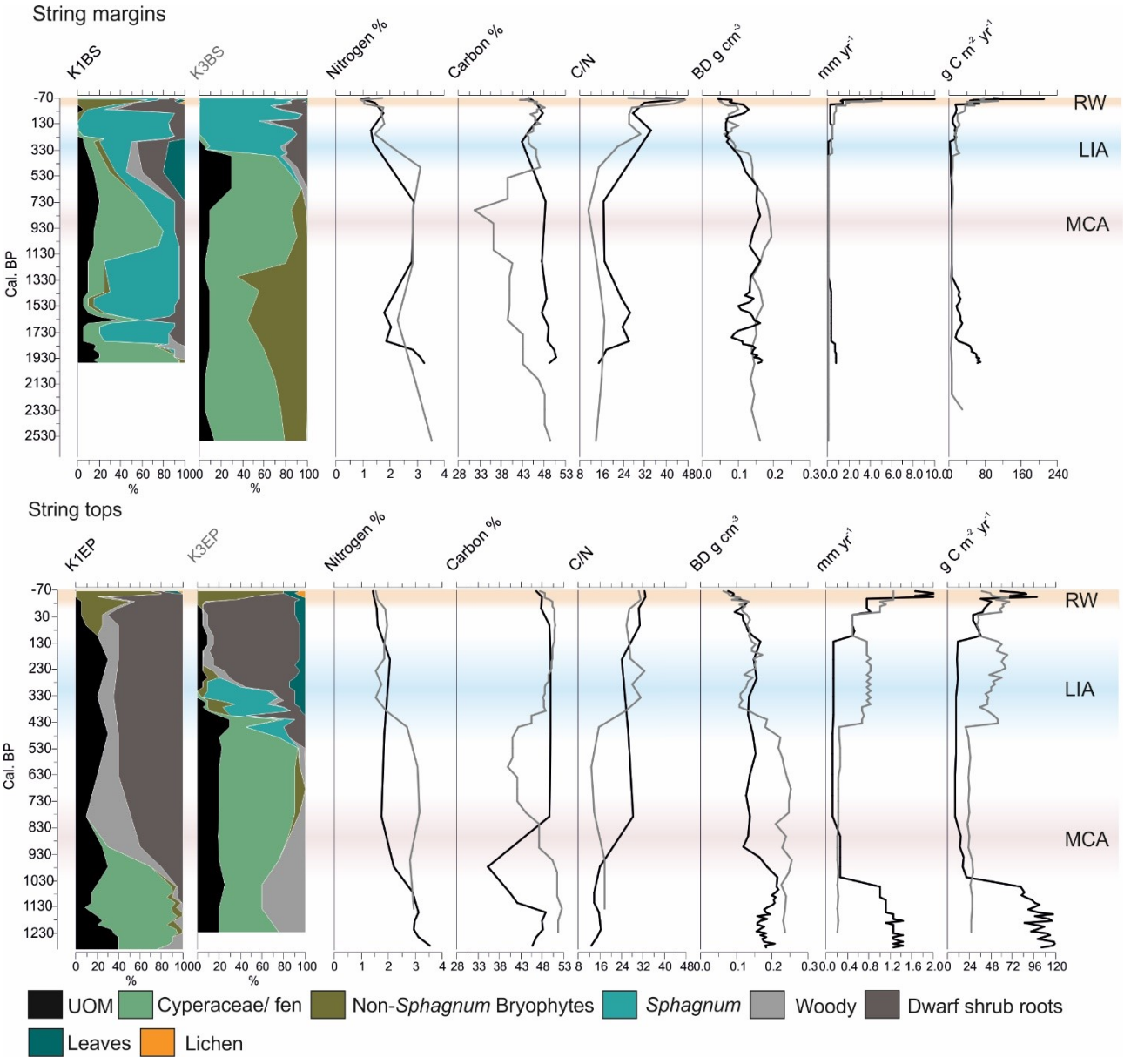

Figure 4. Short string margin records K1BS, K3BS and string top records K1EP, K3EP. Abundance of selected vegetation assemblages (%). Black lines for K1 and grey lines for K3 records. Organic content as loss on ignition (LOI%), dry bulk density (BD g cm^{-3}), peat growth rate (mm yr^{-1}), apparent C accumulation rate (g m^{-2} yr^{-1}). Climate phases (approximate cal. BP), Recent warming (RW), Little Ice Age (LIA) and Medieval Climate Anomaly (MCA) are indicated with different colours.

3.3 Plant community changes and lateral expansion through peatland development

In addition to the four community types of the prevailing vegetation inside the EC footprint, we identified three other plant community types from the historical assemblages. Peat started to form in the basin ca. 10,000 cal. BP (Figure 5). Based on plant macrofossil analyses and sediment properties overall, the southern part of the present peatland area represented aquatic habitat in the beginning. Limnotelmatic *Equisetum fluviatile* dominated vegetation prevailed in the middle section, but in a small ca. 2.5 ha area in the north, peat started to form directly on top of the mineral soil (Figure 5). Between ca. 9000 and 8000 cal. BP aquatic habitats changed to *Equisetum* - Cyperaceae dominated habitats and the total area of the peatland increased from 27 ha and to 31 ha (Figure 5). Between ca. 5000 and 4000 cal. BP peat extent was ca. 40 ha. *Equisetum* habitats disappeared after ca. 4000 cal. BP, after which Cyperacous fen habitats dominated the entire peatland for ca. 3000 years. The northernmost part of the peatland established via primary paludification which took place ca. 2000 cal. BP. Young and shallow peat was also found in the south, close to the basal peat coring point number 17, where the peat initiated between 4000 and 3000 cal. BP. Peat area reached the current 43 ha between ca. 2000 and 1000 cal. BP. Surface microtopoghraphy with high strings and wet flarks formed after ca. 1000 cal. BP creating the present day strongly patterned features.

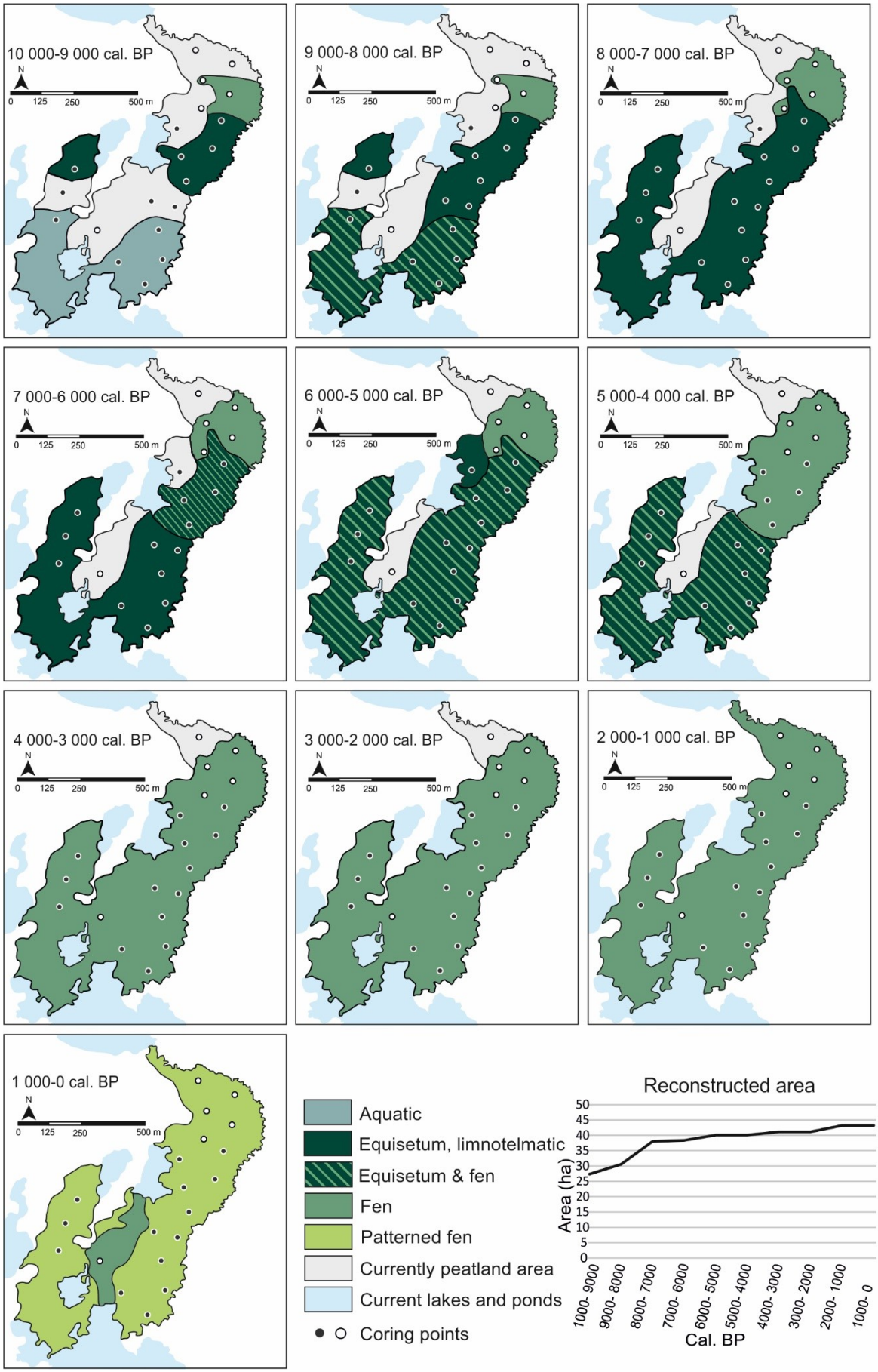
10 000-9 000 cal. BP
9 000-8 000 cal. BP
8 000-7 000 cal. BP
7 000-6 000 cal. BP
6 000-5 000 cal. BP
5 000-4 000 cal. BP
4 000-3 000 cal. BP
3 000-2 000 cal. BP
2 000-1 000 cal. BP
1 000-0 cal. BP
N
0 125 250 500 m
Aquatic
Equisetum, limnotelmatic
Equisetum & fen
Fen
Patterned fen
Currently peatland area
Current lakes and ponds
Coring points
Reconstructed area
Area (ha)
0 5 10 15 20 25 30 35 40 45 50
1000- 9000
9000- 8000
8000- 7000
7000- 6000
6000- 5000
5000- 4000
4000- 3000
3000- 2000
2000- 1000
1000- 0
Cal. BP

Figure 5. Successional development of habitat distribution in patterned flark fen of Kaamanen peatland. The different colours indicate the main vegetation assemblages in thousand-year time-windows. The areas marked with grey are currently part of the peatland. Coring points with black fill indicates limnotelmatic basal conditions and white fill indicates mineral-peat transition.

3.4 Carbon accumulation

Peat C content, measured from the short sections, was on average 47% and varied between 35% and 53% (Figure 4). The average N content was 2.2% with minimum and maximum contents of 0.9% and 3.5% (Figure 4). C and N contents were stable for the top-most 20 cm for all peat records but fluctuated more in the deeper layers (Figure 4). The diverging C content trends between the deeper sections of K1EP and K3EP was especially conspicuous, considering the close proximity of the coring sites to each other.

C accumulation was, on average, 21 and 15 g C m^{-2} yr^{-1} in the long cores STLong and EPLong, respectively. For the STLong, the CAR continuously increased from the core bottom peaking to the highest values of ca. 29 g C m^{-2} yr^{-1} between ca. 6000–7900 cal. BP (Figure 3). A marked CAR decline of about 15 g C m^{-2} yr^{-1} was observed thereafter around 6000 cal. BP. Only minor CAR changes were detected for the EPLong over time. However, the CAR was low: 7-8 g C m^{-2} yr^{-1} for the surface parts.

CAR varied markedly in the short surface cores, but the overall trend was mainly increasing towards the surface. In the string top cores, CAR averages were 65 g C m^{-2} yr^{-1} (K1EP) and 43 g C m^{-2} yr^{-1} (K3EP) and in the string margin cores they were 37 g C m^{-2} yr^{-1} (K1BS) and 29 g C m^{-2} yr^{-1} (K3BS). In contrast to the long cores, CAR was highest over the recent 20 years, 210 g C m^{-2} yr^{-1} (K1BS) and ca. 100 g C m^{-2} yr^{-1} (K1EP). In K1EP core, highest values of ca. 120 g C m^{-2} yr^{-1} occurred at ca. 1100 cal. BP (Figure 4).

3.5 Radiative forcing

While the estimated instantaneous RF varied during the peatland history, according to both flux scenarios the studied site has had a net cooling impact over the 10,000-yr period after the peatland initiation (Figures 6 and 7). This can be observed from the cumulative RF at the end of the period, which is proportional to the total additional energy in the atmosphere. In both scenarios, for the first ca. 1000 years the total (sum of CO_2 and CH_4) instantaneous RF was close to zero (Figure 7), in Scenario 1 marginally positive and in Scenario 2 negative. In Scenario 1, where aquatic communities prevailed late, the total RF was positive (warming impact) approximately between 9000 and 4000 cal. BP. The total RF turned to negative (cooling impact) after ca. 4000 cal. BP and reached the level of strongest cooling (ca. -10 $\times 10^{-8}$ W m^{-2}) before 1000 cal.

BP. In Scenario 2 that allowed the aquatic Sandy *Equisetum* gradually turn into peat-forming littoral, the total RF was marginally negative between ca. 10,000 and 7000 cal. BP, close to zero between ca. 7000 and 6000 cal. BP, and at ca. 6000 cal. BP it turned marginally positive for ca. 400 yr. Since ca. 5500 cal. BP, the total RF was negative, reaching the minimum of -14 $\times 10^{-8}$ W m^{-2} between ca. 1000 and 200 cal. BP.

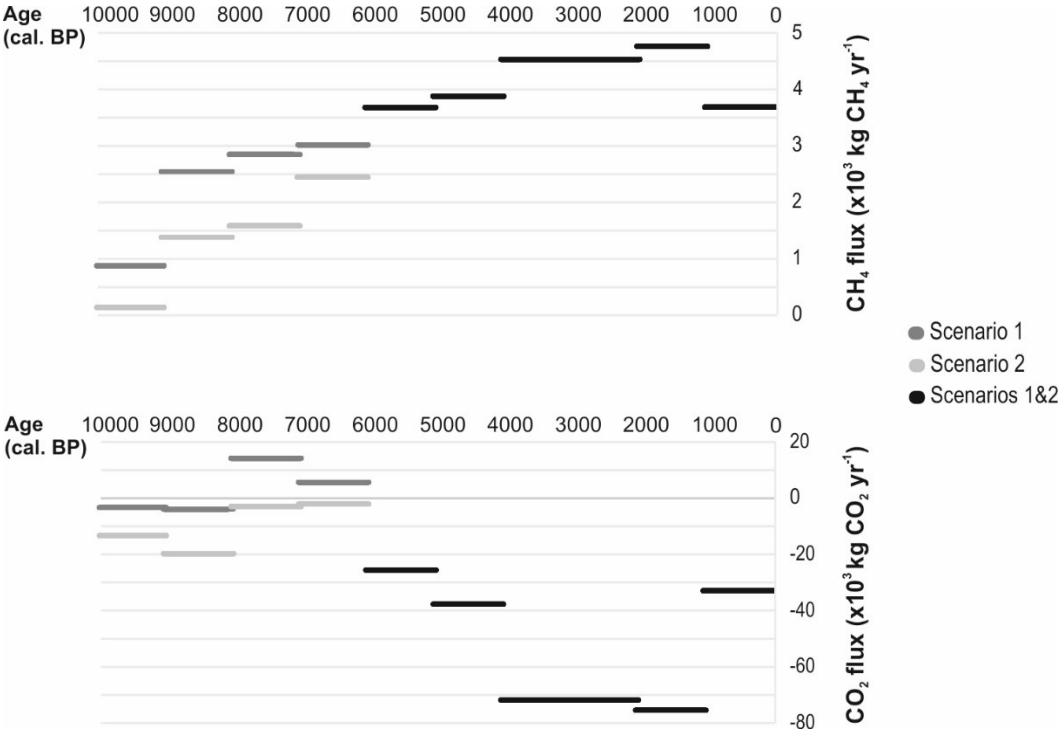

Figure 6. Reconstructed CH_4 and CO_2 flux ($\times 10^3$ kg CH_4 yr^{-1}; $\times 10^3$ kg CO_2 yr^{-1}) scenarios integrated over the total peatland area in Kaamanen peatland over time.

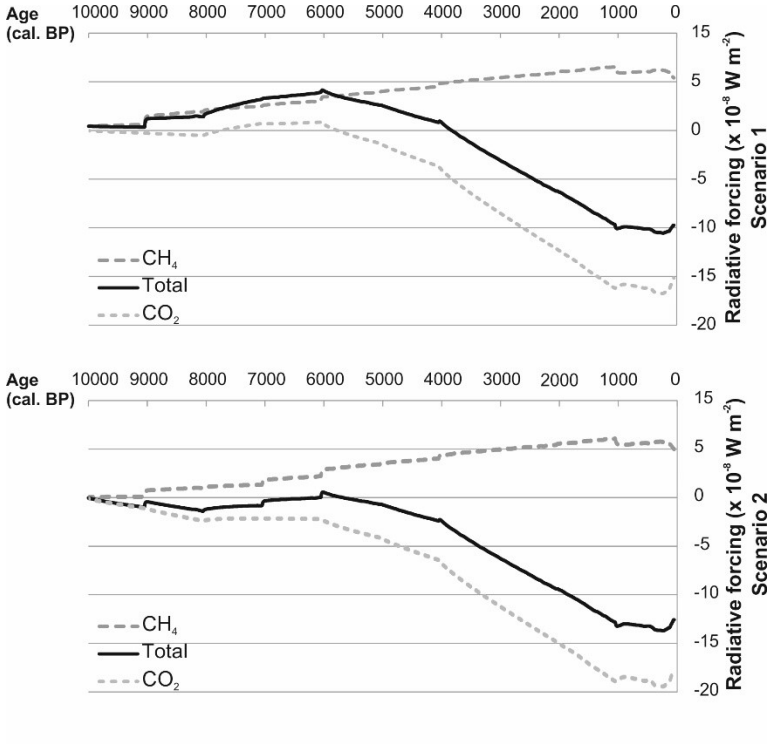

Figure 7. Radiative forcing (RF) due to ecosystem-atmosphere exchange of CO_2 and CH_4 during the succession of the Kaamanen peatland. Two alternative scenarios were created, which differ in their early development from sandy *Equisetum* habitats to peaty *Equisetum*.

4. Discussion

4.1 Peatland initiation and development

The Kaamanen area deglaciated approximately 11,000 cal. BP (Kujansuu 1992; Kujansuu et al., 1998)), which left behind several melt water lakes that were gradually filled in by organic sediments, some rapidly changing to peatlands via terrestrialization. Our data suggest that the studied peatland formed soon after the ice margin withdrawal. In the southern part of the peatland, open water conditions with rather lush vegetation persisted until at least approximately 9500 cal. BP, after which the lake infilling took place. In the middle section of the present peatland area, limnotelmatic peat with abundant *Equisetum* suggests terrestrialization of the shallow littoral lake areas. In the north, peat started to form directly on top of the mineral soil as indicated by a sharp transitional contact from sand to peat. It appears that post-glacial lake – stream landscape processes triggered and regulated the peatland development and expansion. The peatland development in Kaamanen follows acknowledged theories (e.g. Foster and Wright Jr., 1990) of peatland formation beginning at several locations, later combining into a single complex and simultaneously growing both vertically and laterally.

391 The intensive development and expansion of the studied peatland during the early Holocene agrees with earlier studies
392 from the high latitudes, which have revealed that the most rapid expansion period of peatlands occurred during ca. 10,000
393 to 8000 cal. BP (Mäkilä and Moisanen, 2007; Weckström et al., 2010). After the rapid early Holocene paludification, the
394 lateral growth continued with slow a rate following landscape topography, including peat formation directly on mineral
395 soil. This agrees with Weckström et al. (2010), who found only modest lateral expansion from 8000 to 4000 cal. BP.

396 Horizontally, peat started to accumulate relatively simultaneously all over the studied area, but the vertical peat growth
397 rate differed greatly. The landscape is sloping from the north towards the lake in the south, and this may have created the
398 current pattern where the peat deposit thickness is 1 to 2 m in the north, while it is up to 4 m in the south. The original
399 altitudinal difference of 3 m has been evened to a 1 m difference, as the peat growth rate has been twice as high in the
400 south as in the north. In the northern part, measured from EPLong, the long-term average CAR of 15 g C m^2 yr^{-1} is in line
401 with the average estimated for subarctic fens in Finland, 16.9 g C m^2 yr^{-1} (Turunen et al., 2002). In the southern part,
402 however, the CAR average of 21 g C m^2 yr^{-1} from STLong is more comparable with the average accumulation of raised
403 bogs in southern Finland, 23.4 g C m^2 yr^{-1} (Turunen et al., 2002). Probably the initial infilling lake received more nutrients
404 from the surrounding catchment resulting in higher peat and C accumulation rates in the southern core (cf. Mäkilä and
405 Moisanen 2007). Overall, the long-term CAR values are of the same magnitude than the mean Holocene values of
406 northern peatlands, 18.6 g C m^2 yr^{-1} (Yu et al., 2009), 22.9 g C m^2 yr^{-1} (Loisel et al., 2014) and of west Siberian peatlands
407 17.2 6 g C m^2 yr^{-1} (Turunen et al., 2011). Considerable spatial variation in the average long-term CAR within a peatland
408 is not unprecedented as suggested by studies with multiple study points (Mathijssen et al., 2017, 2016; Pelletier et al.,
409 2017; Piilo et al., 2019; Watson et al., 2015; Zhang et al., 2018a). Our data thus highlight the need for multiple study
410 points per site, instead of the common single study-point approach, to reconstruct peatland development and CAR
411 comprehensively and properly estimate basin-wide average rates.

412 *4.2 Peatland response to Holocene climate variation and corresponding radiative forcing*

413 In northern Fennoscandia, **the early Holocene was relatively warm** (Luoto et al., 2014; Väliranta et al., 2015). In
414 Kaamanen, the initial aquatic littoral habitat changed into a peat forming *Equisetum* habitat. The CARs between 20-28 g
415 C m^2 yr^{-1} and 12-18 C m^2 yr^{-1} determined for STLong and EPLong, respectively, are in line with previous studies (Mäkilä
416 and Moisanen, 2007; Mathijssen et al., 2014). For the early limnotelmatic habitat type, we applied two CO_2 and CH_4 flux
417 scenarios to create RF trajectories. Here, we were able to apply the fluxes measured on nearby limnotelmatic *Equisetum*-
418 dominated subarctic fen assemblages (Juutinen et al., 2013), but it should be noted that only a few flux measurements
419 from such ecosystem transitions are available and this uncertainty in our assumptions needs to be taken into account when

interpreting the created RF scenarios. It appeared that the fluxes were relatively low during the first millennium, and thus both scenarios suggested a negligible RF for this period. The system was a small C sink when there were sandy sediments and a net source of C to the atmosphere when organic sediments were deposited. We interpret the latter to result from the release of excess C relative to the on-site C fixation, potentially due to lateral transport of organic matter at the peatland-lake edge (i.e. particulate and dissolved organic C (DOC) transfer from the peatland). This results in a discrepancy: peat record indicates C accumulation, while the applied C exchange rates, which we cannot retrospectively verify, indicate a release of C also in the form of CO_2. This is a feature found within littoral vegetation (Larmola et al., 2003) and, in larger scale, material of terrestrial origin may turn lakes net heterotrophic and CO_2 sources (Cole et al., 1994).

Mid-Holocene was warm and dry (Eronen et al., 1999; Seppä et al., 2009). The STLong record showed strongly decreased C accumulation rates (from 33 to 15 g C m^2 yr^{-1}) after 6000 cal. BP with a simultaneous change from the *Equisetum* characterized assemblages to non-patterned fen vegetation. Similar mid-Holocene decrease in the peat and C accumulation (from 26 to 9 g C m^2 yr^{-1}) and lateral expansion rates have been detected in western Finnish Lapland (Mäkilä and Moisanen, 2007; Mathijssen et al. 2014). The RF Scenario 1, which allowed the aquatic habitat to prevail only for the first 1000-yr. period, showed a warming impact starting from ca. 9000 cal. BP. Scenario 2, with interpolation from the sandy littoral habitat to the littoral peaty *Equisetum* peat habitat, suggested a consistent cooling impact apart from a 400-yr-long period of marginal warming at around 6000 cal. BP. Our results show a notable decrease in lateral expansion already after 7000 cal. BP, and both RF scenarios suggest that the highest positive forcing took place at 6000 cal. BP, after which RF turned to a decreasing trend, with a negative forcing in Scenario 2.

Between 5000 and 3000 cal. BP, i.e. in **the cooler and moister late Holocene** (Seppä and Birks, 2001), our results suggest only minor changes in the vegetation, lateral expansion and CAR. Yet, the RF Scenario 1 suggests positive forcing changing to negative only after 4000 cal. BP. The overall RF pattern, however, supports the prevailing understanding of a peatland ecosystem first having a warming impact that later turns to cooling. The switchover to cooling should be inevitable at some point, as part of the cooling effect due to sustained CO_2 uptake accumulates monotonously while the positive RF due to a continuous CH_4 emission saturates in a few decades.

In contrast to the prevailing consensus and our results, the reconstructed RF of another subarctic fen, located ca. 180 km southeast of our study site, suggested a slight warming effect throughout its 10,000-yr development, even though it has continuously accumulated C (Mathijssen, 2016). Compared to our study site, that fen is shallower, with the maximum peat depth of 2.5 m, and has a more even surface topography, it supports different (tall sedge) vegetation and differs in its historical vegetation succession (Mathijssen et al., 2014). The RF scenarios for a southern Finnish boreal bog suggested

449 a positive forcing for the first 7000 yr. resembling our Scenario 1, even though with a longer phase of positive forcing,
450 reflecting its long-lasting succession from a fen to a bog (Mathijssen et al., 2017). However, Mathijssen et al. (in prep.)
451 demonstrated that the timing of warming-to-cooling switchover is sensitive to model input, i.e. the estimated flux densities
452 and the reconstructed peat area.

453 While the STLong record revealed C accumulation features and changes in vegetation assemblages that seemed to reflect
454 Holocene climate variations, especially mid-Holocene decreased CAR, the other Holocene section EPLong record
455 indicated much more subtle changes in vegetation and accumulation patterns. In other words, no clear and consistent
456 peatland-scale response to warm climate was detected. However, this is possibly due to the age-depth model, which is
457 based on fewer dated levels than STLong, but also to the topographical differences.

458 The detected vegetation succession, from *Equisetum* to Cyperaceae dominated vegetation and further to patterned fen, is
459 also reported for other northern fens (Mäkilä et al., 2001; Mäkilä and Moisanen, 2007). The formation of surface
460 microtopography with strings and flarks has been dated to the **late Holocene,** 3000–2000 cal. BP, elsewhere in Lapland
461 (Mäkilä and Moisanen, 2007; Seppälä and Koutaniemi, 1985). The current understanding is that the origin of
462 microtopography of the raised bogs and fens in Fennoscandia is probably a **large-scale cooling** of the climate and a
463 related **increase in effective humidity** (Aartolahti, 1967; Karofeld, 1998; Mäkilä and Moisanen, 2007; Seppälä and
464 Koutaniemi, 1985). The irregular string and flark pattern, now characteristic of the Kaamanen peatland, was formed only
465 after ca. 1000 cal. BP. These formation processes were dated to both the **warm MCA** (Diaz et al., 2011; Linderholm et
466 al., 2018) and the **cool LIA** (Cook et al., 2004; Hanhijärvi et al., 2013)**.** While the MCA and LIA temperature patterns for
467 European high-latitudes are relatively well resolved, the perception of hydrological conditions for these climate phases
468 vary more (Diaz et al., 2011; Linderholm et al., 2018). Recent peatland hydrological reconstruction for Finnish Lapland,
469 however, suggest relatively dry conditions for both periods (Zhang et al., 2018b), although these data originates from
470 permafrost peatlands, which are more complicated systems. The dry string top in K1EP formed during the early MCA
471 with a simultaneous decrease in CAR. However, the formation of string margin conditions in K1BS, K3BS and K3EP
472 and the following change to dry Ericales-*Pleurozium* community of K3EP occurred during the LIA. The changes dated
473 to the LIA could reflect ice- and frost-related winter processes, which cause movement of unstable landforms
474 (Koutaniemi, 1999). String formation reduced the CO_2 uptake of the fen and halted the decreasing RF trend, as CO_2
475 exchange is associated to fen microtopography and the related variability in plant communities: minerotrophic
476 communities act as effective sinks, while net CO_2 fluxes are smaller in ombrotrophic string top communities (Heikkinen
477 et al., 2002; Maanavilja et al., 2011; Heiskanen et al., 2020).

In our string top and string margin records, CAR was consistently low during the MCA, a pattern also reported for other permafrost-influenced subarctic fens (Zhang et al., 2018a). In the string top K3EP and string margin K3BS records, CAR and *Sphagnum* prevalence seemed to increase during the LIA, which contradicts previous observations of decreased CAR in more southern peatlands during the LIA period (Charman et al., 2013). However, in subarctic permafrost fens higher CAR was detected during the LIA corresponding to our results (Zhang et al., 2018a) and highlighting the importance of *Sphagna* in peatland C dynamics (e.g. Loisel and Yu, 2013). The long records suggested decreasing CARs for the LIA period, but for these two records, the chronology without ^{210}Pb dating is less reliable for the recent centuries. The CARs of the past decades, including **the recent warming** since the 1980s, are high, which is at least partly due to the incomplete decay process, and thus they cannot be directly compared with the older sections (Alm et al., 1999; Clymo et al., 1998; Tolonen and Turunen, 1996; Young et al., 2019). However, a modelling exercise for permafrost-influenced fens suggests that the recent warming has increased the peatland C sink capacity even when the decomposition processes are considered (Zhang et al., 2018a). High peat and C accumulation rates were also detected before the MCA for the K1EP and K1BS records (ca. 110 and 80 g C m^2 yr^{-1}, respectively). This pattern was not related to incomplete decay, nor especially warm climate, but probably reflects a vegetation succession from a wet fen habitat to string margin (K1BS) and string top vegetation (K1EP); this change was then followed by a decrease in CAR.

5. Conclusions and future implications

In this study, the warm climate periods did not seem to result in uniform responses in carbon accumulation rates (CAR) nor vegetation patterns, but vegetation succession appeared to drive changes in CAR and RF more. The overall balance between gross ecosystem productivity and C loss through decomposition and DOC (Roulet et al., 2007) is a complex mixture of forcing factors and, as it is also strongly influenced by site-specific characteristics, the differentiation is challenging. In the future, warmer springs with earlier snowmelt will probably benefit annual CO_2 uptake (Aurela et al., 2004). However, recent ecosystem-scale field experiments have shown that, instead of a direct impact of temperature *per se*, peatland water table is the major driving factor for fen CO_2 dynamics (Laine et al., 2019) and CH_4 emissions (Peltoniemi et al., 2016) as well as for vegetation composition and biomass production (Mäkiranta et al., 2018).

High water tables support peat accumulation by maintaining anoxic conditions in the peat profile, thus slowing decomposition (e.g. Belyea, 1996), while temperature and light conditions, in turn, may restrict net C accumulation (Charman et al., 2013). Our study supports the prevailing understanding of northern peatlands acting as important long-term C sinks with climate cooling feedbacks. However, a widespread drying of European peatlands over the recent past has been suggested (Swindles et al., 2019; Zhang et al., 2020, 2018b). A water level drawdown experiments have shown

that in high latitudes shrubs benefit over forbs and mosses as belowground production increases under drier conditions (Mäkiranta et al., 2018). In addition, changes in vegetation composition may occur fast: drainage of a boreal fen resulted in a rapid shift of *Carex* dominated fen vegetation to *Sphagnum* dominated ombrotrophic communities (Tahvanainen, 2011). Consequently, should the future warming be accompanied by summer water deficiency (Charman, 2007) and lowered water levels, significant changes in fen plant functional types (Mäkiranta et al., 2018) and thus in C accumulation and the related RF may occur.

6. Acknowledgements

We thank O. Kuuri-Riutta, J-P. Manner and M. Amesbury for fieldwork assistance. Academy of Finland (CAPTURE, 296423) funded this project.

7. Author contribution

AK, MV, MA, J-PT and SP designed the research. SP, LH, MV, JT, SJ, HM and MS carried out the fieldwork. SP performed the laboratory analysis under supervision from MV. J-PT, MA, E-ST and LH contributed and modelled the flux data. All authors substantially contributed to the final manuscript.

8. References

Aartolahti, T., 1967. On dating the genesis of peat banks and hollows in the raised bogs of southwestern Finland. Bulletin de la Commission de la Societe Geologie de Finlande 34, 71–86.

Alm, J., Schulman, L., Walden, J., Nykänen, H., Martikainen, P.J., Silvola, J., 1999. Carbon balance of a Boreal bog during a year with an exceptionally dry summer. Ecology 80, 161–174. https://doi.org/https://doi.org/10.1890/0012-9658(1999)080[0161:CBOABB]2.0.CO;2

Appleby, P.G., Oldfield, F., 1978. The calculation of lead-210 dates assuming a constant rate of supply of unsupported 210 Pb to the sediment. Catena 5, 1–8.

Aurela, M., Laurila, T., Tuovinen, J., 2001. Seasonal CO2 balances of a subarctic mire downward flux densities at the end while the highest respiration rates observed later through the snow cover was about -l . In correspondence m were observed in July . The highest positive balances of about m peri. Quality 106, 1623–1637.

Aurela, M., Laurila, T., Tuovinen, J.P., 2004. The timing of snow melt controls the annual CO2 balance in a subarctic fen. Geophys. Res. Lett. 31, 3–6. https://doi.org/10.1029/2004GL020315

Aurela, M., Laurila, T., Tuovinen, J.P., 2002. Annual CO2 balance of a subarctic fen in northern Europe: Importance of the wintertime efflux. J. Geophys. Res. Atmos. 107, 1–12. https://doi.org/10.1029/2002JD002055

Aurela, M., Tuovinen, J.P., Laurila, T., 1998. Carbon dioxide exchange in a subarctic peatland ecosystem in northern Europe measured by the eddy covariance technique. J. Geophys. Res. Atmos. 103, 11289–11301. https://doi.org/10.1029/98JD00481

Belyea, L.R., 1996. Separating the Effects of Litter Quality and Microenvironment on Decomposition Rates in a Patterned Peatland. Nord. Soc. Oikos 77, 529–539.

Blaauw, M., 2010. Methods and code for "classical" age-modelling of radiocarbon sequences. Quat. Geochronol. 5, 512–518. https://doi.org/10.1016/j.quageo.2010.01.002

Blaauw, M., Christen, J.A., 2011. Flexible paleoclimate age-depth models using an autoregressive gamma process. Bayesian Anal. 6, 457–474. https://doi.org/10.1214/11-BA618

Boucher, O., Friedlingstein, P., Collins, B., Shine, K.P., 2009. The indirect global warming potential and global temperature change potential due to methane oxidation. Environ. Res. Lett. 4. https://doi.org/10.1088/1748-9326/4/4/044007

Box, J.E., Colgan, W.T., Christensen, T.R., Schmidt, N.M., Lund, M., Parmentier, F.-J.W., Brown, R., Bhatt, U.S., Euskirchen, E.S., Romanovsky, V.E., Walsh, J.E., Overland, J.E., Wang, M., Corell, R.W., Meier, W.N., Wouters, B., Mernild, S., Mård, J., Pawlak, J., Olsen, M.S., 2019. Key indicators of Arctic climate change: 1971–2017. Environ. Res. Lett. 14, 045010. https://doi.org/10.1088/1748-9326/aafc1b

Charman, D.J., Beilman, D.W., Blaauw, M., Booth, R.K., Brewer, S., Chambers, F.M., Christen, J.A., Gallego-Sala, A., Harrison, S.P., Hughes, P.D.M.M., Jackson, S.T., Korhola, A., Mauquoy, D., Mitchell, F.J.G.G., Prentice, I.C., Van Der Linden, M., De Vleeschouwer, F., Yu, Z.C., Alm, J., Bauer, I.E., Corish, Y.M.C.C., Garneau, M., Hohl, V., Huang, Y., Karofeld, E., Le Roux, G., Loisel, J., Moschen, R., Nichols, J.E., Nieminen, T.M., MacDonald, G.M., Phadtare, N.R., Rausch, N., Sillasoo, U., Swindles, G.T., Tuittila, E.S., Ukonmaanaho, L., Väliranta, M., Van Bellen, S., Van Geel, B., Vitt, D.H., Zhao, Y., 2013. Climate-related changes in peatland carbon accumulation during the last millennium. Biogeosciences 10, 929–944. https://doi.org/10.5194/bg-10-929-2013

Charman, D.J., 2007. Summer water deficit variability controls on peatland water-table changes: Implications for Holocene palaeoclimate reconstructions. Holocene 17, 217–227. https://doi.org/10.1177/0959683607075836

Clymo, A.R.S., Turunen, J., Tolonen, K., 1998. Carbon accumulation in peatland. Nord. Soc. Oikos 81, 368–388.

Cole, J.J., Caraco, N.F., Kling, G.W., Kratz, T.K., 1994. Carbon Dioxide Supersaturation in the Surface Waters of Lakes. Science (80-.). 265, 1568–1570. https://doi.org/10.1126/science.265.5178.1568 ARTICLE

Collins, M., Knutti, R., Arblaster, J., Dufresne, J.-L., Fichefet, T., Friedlingstein, P., Gao, X., Gutowski, W.J., Johns, T., Krinner, G., Shongwe, M., Tebaldi, C., Weaver, A.J., Wehner, M., 2013. Long-term Climate Change: Projections, Commitments and Irreversibility, in: Stocker, T.F., Qin, D., Plattner, G.-K., Tignor, M., Allen, S.K., Boschung, J., Nauels, A., Xia, Y., Bex, V., Midgley, P.M. (Eds.) Clim. Chang. 2013 Phys. Sci. Basis. Contrib. Work. Gr. I to Fifth Assess. Rep. Intergov. Panel Clim. Chang. Cambridge University Press, Cambridge, United Kingdom and

New York, NY, USA.

Cook, E.R., Esper, J., Arrigo, R.D.D., 2004. Extra-tropical Northern Hemisphere land temperature variability over the past 1000 years. Quat. Sci. Rev. 23, 2063–2074. https://doi.org/10.1016/j.quascirev.2004.08.013

Diaz, H.F., Trigo, R., Hughes, M.K., Mann, M.E., Xoplaki, E., Barriopedro, D., 2011. Spatial and temporal characteristics of climate in medieval times revisited. Am. Meteorol. Soc. 92, 1487–1500. https://doi.org/10.1175/2011bams-d-10-05003.1

Eronen, M., Hyvärinen, H., Zettenberg, P., 1999. Holocene humidity changes in northern Finnish Lapland inferred from lake sediments and submerged Scots pines dated by tree-rings. The Holocene 9, 569–580.

Estop-Aragonés, C., Cooper, M.D.A., Fisher, J.P., Thierry, A., Garnett, M.H., Charman, D.J., Murton, J.B., Phoenix, G.K., Treharne, R., Sanderson, N.K., Burn, C.R., Kokelj, S. V., Wolfe, S.A., Lewkowicz, A.G., Williams, M., Hartley, I.P., 2018. Limited release of previously-frozen C and increased new peat formation after thaw in permafrost peatlands. Soil Biol. Biochem. 118, 115–129. https://doi.org/10.1016/j.soilbio.2017.12.010

Etminan, M., Myhre, G., Highwood, E.J., Shine, K.P., 2016. Radiative forcing of carbon dioxide, methane, and nitrous oxide: A significant revision of the methane radiative forcing. Geophys. Res. Lett. 43, 614–623. https://doi.org/10.1002/2016GL071930

Eurola, S., Bendiksen, K., Rönkä, A., 1992. Suokasviopas. 2. korjattu painos. Oulanka Reports, Viramo, J., (Eds.) Oulanka Biological Station, University of Oulu, Finland

Foster, D.R., Wright Jr., H.E., 1990. Role of Ecosystem Development and Climate Change in Bog Formation in Central Sweden. Ecology 71, 450–463.

Frolking, S., Roulet, N.T., 2007. Holocene radiative forcing impact of northern peatland carbon accumulation and methane emissions. Glob. Chang. Biol. 13, 1079–1088. https://doi.org/10.1111/j.1365-2486.2007.01339.x

Gałka, M., Swindles, G.T., Szal, M., Fulweber, R., Feurdean, A., 2018. Response of plant communities to climate change during the late Holocene: Palaeoecological insights from peatlands in the Alaskan Arctic. Ecol. Indic. 85, 525–536. https://doi.org/10.1016/j.ecolind.2017.10.062

Gong, J., Kellomäki, S., Wang, K., Zhang, C., Shurpali, N., Martikainen, P.J., 2013. Modeling CO2 and CH4 flux changes in pristine peatlands of Finland under changing climate conditions. Ecol. Modell. 263, 64–80. https://doi.org/10.1016/j.ecolmodel.2013.04.018

Gorham, E., 1991. Northern Peatlands : Role in the Carbon Cycle and Probable Responses to Climatic Warming. Ecol. Appl. 1, 182–195. https://doi.org/10.2307/1941811

Grimm, E.C., 1991. TILIA and TILIAGRAPH Software. Springfield, Illinois.

Hanhijärvi, S., Tingley, M.P., Korhola, A., 2013. Pairwise comparisons to reconstruct mean temperature in the Arctic Atlantic Region over the last 2 , 000 years. Clim. Dyn. 41, 2039–2060. https://doi.org/10.1007/978-1-4020-2121-3

Hargreaves, K.J., Fowler, D., Pitcairn, C.E.R., Aurela, M., 2001. Annual methane emission from Finnish mires estimated from eddy covariance campaign measurements. Theor. Appl. Climatol. 70, 203–213. https://doi.org/10.1007/s007040170015

Heikkinen, J.E.P., Maljanen, M., Aurela, M., Hargreaves, K.J., Martikainen, P.J., 2002. Carbon dioxide and methane dynamics in a sub-Arctic peatland in northern Finland. Polar Res. 21, 49–62. https://doi.org/10.1111/j.1751-8369.2002.tb00066.x

Helbig, M., Waddington, J.M., Alekseychik, P., Amiro, B., Aurela, A., Barr, A.G., Black, T.A., Blanken, P.D., Carey, S.K., Chen, J., Chi, J., Desai, A.R., Dunn, A., Euskirchen, E., Friborg, T., Flanagan, L.B., Forbrich, I., Grelle, A., Harder, S., Heliasz, M., Humphreys, E.R., Ikawa, H., Iwata, H., Isabelle, P-E., Jassal, R., Kurbatova, J., Korkiakoski, M., Kutzbach, L., Ohta, T., Lindroth, A., Ottosson, Löfvenius, M., Lohila, A., Maksimov, T., Mammarella, I., Marsh, P., Melton, J.R., Moore, P.A., Nadeau, D., Nicholls, E.M., Nilsson, M.B., Peichl, M., Petrone, R.M., Petrov, R., Quinton, W., Roulet, N., Reed, D., Runkle, B.R.K., Rutgersson, A., Sahlee, E., Sonnentag, O., Strachan, IB., Taillardat, B, Tuittila, E-S., Tuovinen, J-P., Turner, J., Ueyama, M., Varlagin, A., Wilmking, M., Wofsy, S., 2020. Increasing contribution of peatlands to boreal evapotranspiration in a warming climate. Nat. Clim. Chang. https://doi.org/10.1038/s41558-020-0763-7

Heiri, O., Lotter, A.F., Lemcke, G., 2001. Loss on ignition as a method for estimating organic and carbonate content in

617 sediments: reproducibility and comparability of results. J. Paleolimnol. 25, 101–110.

618 Heiskanen, L., Tuovinen, J.-P., Räsänen, A., Virtanen T., Juutinen S., Penttilä, T., Mikola, J., Linkosalmi, M., Laurila,
619 T., Aurela M., 2020. Carbon dioxide and methane exchange of a patterned subarctic fen during two contrasting
620 growing seasons. Biogeosciences, Submitted.

621 Holmquist, J.R., Finkelstein, S.A., Garneau, M., Massa, C., Yu, Z., MacDonald, G.M., 2016. A comparison of
622 radiocarbon ages derived from bulk peat and selected plant macrofossils in basal peat cores from circum-arctic
623 peatlands. Quat. Geochronol. 31. https://doi.org/10.1016/j.quageo.2015.10.003

624 Howard, A.J., Gearey, B.R., Hill, T., Fletcher, W., Marshall, P., 2009. Fluvial sediments, correlations and
625 palaeoenvironmental reconstruction: The development of robust radiocarbon chronologies. J. Archaeol. Sci. 36,
626 2680–2688. https://doi.org/10.1016/j.jas.2009.08.006

627 IPCC, 2013. Summary for policymakers, in: Stocker, T.F., Qin, D., Plattner, G.-K., Tignor, M., Allen, S. K., Boschung,
628 J., Nauels, A., Xia, Y., Bex, V., Midgley, P.M. (Eds.), Clim. Chang. 2013 Phys. Sci. Basis. Contrib. Work. Gr. I
629 to Fifth Assess. Rep. Intergov. Panel Clim. Chang. Cambridge University Press, Cambridge, United Kingdom and
630 New York, NY, USA.

631 Jaatinen, K., Fritze, H., Laine, J., Laiho, R., 2007. Effects of short- and long-term water-level drawdown on the
632 populations and activity of aerobic decomposers in a boreal peatland. Glob. Chang. Biol. 13, 491–510.
633 https://doi.org/10.1111/j.1365-2486.2006.01312.x

634 Juggins, S., 2007. C2 user guide: Software for ecological and palaeoecological data analysis and visualization. Univ.
635 Newcastle, Newcastle upon Tyne, UK 1–73.

636 Juutinen, S., Väliranta, M., Kuutti, V., Laine, A.M., Virtanen, T., Seppä, H., Weckström, J., Tuittila, E.S., 2013. Short-
637 term and long-term carbon dynamics in a northern peatland-stream-lake continuum: A catchment approach. J.
638 Geophys. Res. Biogeosciences 118, 171–183. https://doi.org/10.1002/jgrg.20028

639 Karofeld, E., 1998. The dynamics of the formation and development of hollows in raised bogs in Estonia. Holocene 8,
640 697–704. https://doi.org/10.1191/095968398677584475

641 Kelly, T.J., Lawson, I.T., Roucoux, K.H., Baker, T.R., Jones, T.D., Sanderson, N.K., 2017. The vegetation history of an
642 Amazonian domed peatland. Palaeogeogr. Palaeoclimatol. Palaeoecol. 468, 129–141.
643 https://doi.org/10.1016/j.palaeo.2016.11.039

644 Köhler, P., Nehrbass-ahles, C., Schmitt, J., Stocker, T.F., Fischer, H., 2017. A 156 kyr smoothed history of the
645 atmospheric greenhouse gases CO 2 , CH 4 , and N 2 O and their radiative forcing. Earth Syst. Sci. Data 9, 363–
646 387. https://doi.org/https://doi.org/10.5194/essd-9-363-2017

647 Kokkonen, N.A.K., Laine, A.M., Laine, J., Vasander, H., Kurki, K., Gong, J., Tuittila, E., 2019. Journal of Vegetation
648 Science Responses of peatland vegetation to 15 - year water level drawdown as mediated by fertility level. J. Veg.
649 Sci. 30, 1206–1216. https://doi.org/10.1111/jvs.12794

650 Korhola, A., 1994. Radiocarbon evidence for rates of lateral expansion in raised mires in southern Finland. Quat. Res.
651 42, 299–307. https://doi.org/https://doi.org/10.1006/qres.1994.1080

652 Korhola, A., Alm, J., Tolonen, K., Jungner, H., 1996. Three-dimensional reconstruction of carbon accumulation and
653 CH4 emission during nine millennia in a raised mire. J. Quat. Sci. 11, 161–165.

654 Koutaniemi, L., 1999. Twenty-one years of string movements on the Liippasuo aapa mire, Finland. Boreas 28, 521–
655 530. https://doi.org/10.1111/j.1502-3885.1999.tb00238.x

656 Kujansuu, R., Eriksson, B., Grönlund, T., 1998. Lake Inarijarvi, northern Finland: Sedimentation and late Quaternary
657 evolution. Rep. Investig. Geol. Surv. Finl. 6–25.

658 Kujansuu, R., 1992. The deglaciation of Finnish Lapland. Geological Survey of Finland, Special Paper 15,
659 21-31.

660 Laine, A., Riutta, T., Juutinen, S., Väliranta, M., Tuittila, E.S., 2009. Acknowledging the spatial heterogeneity in
661 modelling/reconstructing carbon dioxide exchange in a northern aapa mire. Ecol. Modell. 220, 2646–2655.
662 https://doi.org/10.1016/j.ecolmodel.2009.06.047

663 Laine, A.M., Mäkiranta, P., Laiho, R., Mehtätalo, L., Penttilä, T., Korrensalo, A., Minkkinen, K., Fritze, H., Tuittila, E.-
664 S., 2019. Warming impacts on boreal fen CO 2 exchange under wet and dry conditions . Glob. Chang. Biol. 1–

14. https://doi.org/10.1111/gcb.14617

Laine, J., Harju, P., Timonen, T., Laine, A., Tuittila, E-S., Minkkinen, K., Vasander, H., 2009. The Intricate Beauty of Sphagnum Mosses – A Finnish Guide to Identification. University of Helsinki Department of Forest Ecology, Publications, Finland.

Larmola, T., Alm, J., Juutinen, S., Martikainen, P.J., Silvola, J., 2003. Ecosystem CO2 exchange and plant biomass in the littoral zone of a boreal eutrophic lake. Freshw. Biol. 48, 1295–1310. https://doi.org/10.1046/j.1365-2427.2003.01079.x

Linderholm, H.W., Nicolle, M., Francus, P., Gajewski, K., Helama, S., Korhola, A., Solomina, O., Yu, Z., Zhang, P., D'Andrea, W.J., Debret, M., Divine, D. V., Gunnarson, B.E., Loader, N.J., Massei, N., Seftigen, K., Thomas, E.K., Werner, J., Andersson, S., Berntsson, A., Luoto, T.P., Nevalainen, L., Saarni, S., Väliranta, M., 2018. Arctic hydroclimate variability during the last 2000 years: Current understanding and research challenges. Clim. Past 14, 473–514. https://doi.org/10.5194/cp-14-473-2018

Lohila, A., Minkkinen, K., Laine, J., Savolainen, I., Tuovinen, J.P., Korhonen, L., Laurila, T., Tietäväinen, H., Laaksonen, A., 2010. Forestation of boreal peatlands: Impacts of changing albedo and greenhouse gas fluxes on radiative forcing. J. Geophys. Res. Biogeosciences 115, 1–15. https://doi.org/10.1029/2010JG001327

Loisel, J., Yu, Z., 2013. Recent acceleration of carbon accumulation in a boreal peatland, south central Alaska. J. Geophys. Res. Biogeosciences 118, 41–53. https://doi.org/10.1029/2012JG001978

Loisel, J., Yu, Z., Beilman, D.W., Camill, P., Alm, J., Amesbury, M.J., Anderson, D., Andersson, S., Bochicchio, C., Barber, K., Belyea, L.R., Bunbury, J., Chambers, F.M., Charman, D.J., De Vleeschouwer, F., Fiałkiewicz-Kozieł, B., Finkelstein, S.A., Gałka, M., Garneau, M., Hammarlund, D., Hinchcliffe, W., Holmquist, J., Hughes, P., Jones, M.C., Klein, E.S., Kokfelt, U., Korhola, A., Kuhry, P., Lamarre, A., Lamentowicz, M., Large, D., Lavoie, M., MacDonald, G., Magnan, G., Mäkilä, M., Mallon, G., Mathijssen, P., Mauquoy, D., McCarroll, J., Moore, T.R., Nichols, J., O'Reilly, B., Oksanen, P., Packalen, M., Peteet, D., Richard, P.J.H., Robinson, S., Ronkainen, T., Rundgren, M., Sannel, a. B.K., Tarnocai, C., Thom, T., Tuittila, E.-S.E.S., Turetsky, M., Väliranta, M., van der Linden, M., van Geel, B., van Bellen, S., Vitt, D., Zhao, Y., Zhou, W., 2014. A database and synthesis of northern peatland soil properties and Holocene carbon and nitrogen accumulation. Holocene 24, 1028–1042. https://doi.org/10.1177/0959683614538073

Luoto, T.P., Kaukolehto, M., Weckström, J., Korhola, A., Väliranta, M., 2014. New evidence of warm early-Holocene summers in subarctic Finland based on an enhanced regional chironomid-based temperature calibration model. Quat. Res. 81, 50–62. https://doi.org/10.1016/j.yqres.2013.09.010

Maanavilja, L., Riutta, T., Aurela, M., Pulkkinen, M., Laurila, T., Tuittila, E.S., 2011. Spatial variation in CO2 exchange at a northern aapa mire. Biogeochemistry 104, 325–345. https://doi.org/10.1007/s10533-010-9505-7

MacDonald, G.M., Beilman, D.W., Kremenetski, K. V., Sheng, Y., Smith, L.C., Velichko, A.A., 2006. Rapid early development of circumarctic peatlands and atmospheric CH4 and CO2 variations. Science 314, 285–288. https://doi.org/10.1126/science.1131722

Mäkilä, M., Moisanen, M., 2007. Holocene lateral expansion and carbon accumulation of Luovuoma, a northern fen in Finnish Lapland. Boreas 36, 198–210. https://doi.org/10.1080/03009480600994460

Mäkilä, M., Saarnisto, M., Kankainen, T., 2001. Aapa Mires as a Carbon Sink and Source during the Holocene Linked references are available on JSTOR for this article : Aapa mires as a carbon sink and source during the Holocene. J. Ecol. 89, 589–599.

Mäkiranta, P., Laiho, R., Mehtätalo, L., Straková, P., Sormunen, J., Minkkinen, K., Penttilä, T., Fritze, H., Tuittila, E.S., 2018. Responses of phenology and biomass production of boreal fens to climate warming under different water-table level regimes. Glob. Chang. Biol. 24, 944–956. https://doi.org/10.1111/gcb.13934

Mann, M.E., Zhang, Z., Rutherford, S., Bradley, R.S., Hughes, M.K., Shindell, D., Ammann, C., Faluvegi, G., Ni, F., 2009. Global Signatures and Dynamical Origins of the Little Ice Age and Medieval Climate Anomaly. Science 326, 1256–1260. https://doi.org/10.1126/science.1166349

Mathijssen, P., Tuovinen, J.P., Lohila, A., Aurela, M., Juutinen, S., Laurila, T., Niemelä, E., Tuittila, E.S., Väliranta, M., 2014. Development, carbon accumulation, and radiative forcing of a subarctic fen over the Holocene. Holocene 24, 1156–1166. https://doi.org/10.1177/0959683614538072

Mathijssen, P.J.H., 2016. Department of Environmental Sciences Holocene Carbon Dynamics And Atmospheric

715 Radiative Forcing of Different Types of Peatlands in Finland. Faculty of Biological and Environmental Sciences
716 Department of Environmental Sciences University of Helsinki Finland, Helsinki, Finland.

717 Mathijssen, P.J.H., Kähkölä, N., Tuovinen, J.P., Lohila, A., Minkkinen, K., Laurila, T., Väliranta, M., 2017. Lateral
718 expansion and carbon exchange of a boreal peatland in Finland resulting in 7000 years of positive radiative
719 forcing. J. Geophys. Res. Biogeosciences 122, 562–577. https://doi.org/10.1002/2016JG003749

720 Mathijssen, P.J.H., Väliranta, M., Korrensalo, A., Alekseychik, P., Vesala, T., Rinne, J., Tuittila, E.S., 2016.
721 Reconstruction of Holocene carbon dynamics in a large boreal peatland complex, southern Finland. Quat. Sci.
722 Rev. 142, 1–15. https://doi.org/10.1016/j.quascirev.2016.04.013

723 Mathijssen, P.J.H., Tuovinen, J.-P., Lohila, A.,Tuittila, E.-S., Väliranta, M. (in prep.). Uncertainties in peatland carbon
724 balance reconstructions affecting past and present radiative forcing.

725 Mauquoy, D., van Geel, B., 2007. Plant macrofossil methods and studies: Mire and Peat Macros. In Elias SA, editor,
726 Encyclopedia of Quaternary Science. Amsterdam, Netherlands: Elsevier Science. p. 2315-
727 2336. https://doi.org/10.1016/B0-44-452747-8/00229-5

728 McGuire, A.D., Lawrence, D.M., Koven, C., Clein, J.S., Burke, E., Chen, G., 2018. Dependence of the evolution of
729 carbon dynamics in the northern permafrost region on the trajectory of climate change. PNAS 1–6.
730 https://doi.org/10.1073/pnas.1719903115

731 Morris, P.J., Swindles, G.T., Valdes, P.J., Ivanovic, R.F., Gregoire, L.J., Smith, M.W., Tarasov, L., Haywood, A.M.,
732 Bacon, K.L., 2018. Global peatland initiation driven by regionally asynchronous warming. Proc. Natl. Acad. Sci.
733 U. S. A. 115, 4851–4856. https://doi.org/10.1073/pnas.1717838115

734 Myhre, G., Shindell, D., Bréon, F.-M., Collins, W., Fuglestvedt, J., Huang, J., Koch, D., Lamarque, J.-F., Lee, D.,
735 Mendoza, B., Nakajima, T., Robock, A., Stephens, G., Takemura, T., Zhang, H., 2013. Anthropogenic and
736 Natural Radiative Forcing, in: Stocker, T.F., Qin, D., Plattner, G.-K., Tignor, M., Allen, S.K., Boschung, J.,
737 Nauels, A., Xia, Y., Bex, V., Midgley, P.M. (Eds.) Clim. Chang. 2013 Phys. Sci. Basis. Contrib. Work. Gr. I to
738 Fifth Assess. Rep. Intergov. Panel Clim. Chang. Cambridge University Press, Cambridge, United Kingdom and
739 New York, NY, USA.

740 Nichols, J.E., Peteet, D.M., 2019. Rapid expansion of northern peatlands and doubled estimate of carbon storage. Nat.
741 Geosci. 1–6. https://doi.org/10.1038/s41561-019-0454-z

742 Pelletier, N., Talbot, J., Olefeldt, D., Turetsky, M., Blodau, C., Sonnentag, O., Quinton, W.L., 2017. Influence of
743 Holocene permafrost aggradation and thaw on the paleoecology and carbon storage of a peatland complex in
744 northwestern Canada. The Holocene 27, 1391–1405. https://doi.org/10.1177/0959683617693899

745 Peltoniemi, K., Laiho, R., Juottonen, H., Bodrossy, L., Kell, D.K., Minkkinen, K., Mäkiranta, P., Mehtätalo, L.,
746 Penttilä, T., Siljanen, H.M.P., Tuittila, E., Tuomivirta, T., Fritze, H., 2016. Responses of methanogenic and
747 methanotrophic communities to warming in varying moisture regimes of two boreal fens. Soil Biol. Biochem. 97,
748 144–156. https://doi.org/10.1016/j.soilbio.2016.03.007

749 Piilo, S.R., Zhang, H., Garneau, M., Gallego-sala, A., Amesbury, M.J., Väliranta, M.M., 2019. Recent peat and carbon
750 accumulation following the Little Ice Age in Recent peat and carbon accumulation following the Little Ice Age in
751 northwestern Québec , Canada. Environ. Res. Lett. 14, 75002. https://doi.org/10.1088/1748-9326/ab11ec

752 Pirinen, P., Simola, H., Aalto, J., Kaukoranta, J.-P., Karlsson, P., Ruuhela, R., 2012. Climatological Statistics of Finland
753 1981–2010., Reports 2012: Finnish Meteorological Institute.

754 Post, E., Alley, R., Christensen, T., Macias-Fauria, M., Forbes, B., Gooseff, M., Iler, A., Kerby, J., Laidre, K., Mann,
755 M., Olofsson, J., Stroeve, J., Ulmer, F., Virginia, R., Wang, M., 2019. The Polar regions in a 2°C warmer world.
756 Sci. Adv. 5, 1–13. https://doi.org/10.1126/sciadv.aaw9883

757 R Development Core Team, 2016. R: A Language and Environment for Statistical Computing. The R Foundation for
758 Statistical Computing, Vienna, Austria

759 Räsänen, A., Juutinen, S., Tuittila, E.S., Aurela, M., Virtanen, T., 2019. Comparing ultra-high spatial resolution remote-
760 sensing methods in mapping peatland vegetation. J. Veg. Sci. 30, 1016–1026. https://doi.org/10.1111/jvs.12769

761 Renssen, H., Seppä, H., Crosta, X., Goosse, H., Roche, D.M., 2012. Global characterization of the Holocene Thermal
762 Maximum. Quat. Sci. Rev. 48, 7–19. https://doi.org/10.1016/j.quascirev.2012.05.022

763 Robinson, S.D., 2006. Carbon accumulation in peatlands, southwestern Northwest Territories, Canada. Can. J. Soil Sci.

86, 305–319. https://doi.org/10.4141/S05-086

Roulet, N.T., Lafleurs, P.M., Richard, P.J.H., Moore, T.R., Humphreys, E.R., Bubier, J., 2007. Contemporary carbon balance and late Holocene carbon accumulation in a northern peatland. Glob. Chang. Biol. 13, 397–411. https://doi.org/10.1111/j.1365-2486.2006.01292.x

Ruppel, M., Väliranta, M., Virtanen, T., Korhola, A., 2013. Postglacial spatiotemporal peatland initiation and lateral expansion dynamics in North America and northern Europe. Holocene 23, 1596–1606. https://doi.org/10.1177/0959683613499053

Sandmeier, K.J., 2016. ReflexW (Computer software). Sandmeier software. https://www.sandmeier-geo.de/

Sannel, A.B.K., Hempel, L., Kessler, A., Prėskienis, V., 2017. Holocene development and permafrost history in sub-arctic peatlands in Tavvavuoma, northern Sweden. Boreas. https://doi.org/10.1111/bor.12276

Seppä, H., Birks, H.J.B., 2001. July mean temperature and annual precipitation trends during the Holocene in the Fennoscandian tree-line area: Pollen-based climate reconstructions. The Holocene 11, 527–539. https://doi.org/10.1191/095968301680223486

Seppä, H., Bjune, A.E., Telford, R.J., Birks, H.J.B., Veski, S., 2009. Last nine-thousand years of temperature variability in Northern Europe. Clim. Past 5, 523–535. https://doi.org/10.5194/cp-5-523-2009

Seppälä, M., Koutaniemi, L., 1985. Formation of a string and pool topography as expressed by morphology, stratigraphy and current processes on a mire in Kuusamo, Finland. Boreas 14, 287–309. https://doi.org/10.1111/j.1502-3885.1985.tb00917.x

Swindles, G.T., Morris, P.J., Mullan, D.J., Payne, R.J., Roland, T.P., Amesbury, M.J., Lamentowicz, M., Turner, T.E., Gallego-sala, A., Sim, T., Barr, I.D., Blaauw, M., Blundell, A., Chambers, F.M., Charman, D.J., Feurdean, A., Galloway, J.M., Gałka, M., Green, S.M., Kajukało, K., Karofeld, E., Korhola, A., Lamentowicz, L., Langdon, P., Marcisz, K., Mauquoy, D., Mazei, Y.A., McKeown, M.M., Mitchell, E.A.D., Novenko, E., Plunkett, G., Roe, H. M., Schoning, K., Sillasoo, Ü., Tsyganov, A.N., van der Linden, M., Väliranta, M., Warner, B., 2019. Widespread drying of European peatlands in recent centuries. Nat. Geosci. https://doi.org/10.1038/s41561-019-0462-z

Tahvanainen, T., 2011. Abrupt ombrotrophication of a boreal aapa mire triggered by hydrological disturbance in the catchment. J. Ecol. 99, 404–415. https://doi.org/10.1111/j.1365-2745.2010.01778.x

Tolonen, K., Turunen, J., 1996. Accumulation rates of carbon in mires in Finland and implications for climate change. The Holocene 6, 171–178.

Turunen, J., Tahvanainen, T., Tolonen, K., 2001. Carbon accumulation in West Siberian mires, Russia. Global Biogeochem. Cycles 15, 285–296. https://doi.org/https://doi.org/10.1029/2000GB001312

Turunen, J., Tomppo, E., Tolonen, K., Reinikainen, A., 2002. Estimating carbon accumulation rates of undrained mires in Finland–application to boreal and subarctic regions. The Holocene 12, 69–80. https://doi.org/10.1191/0959683602hl522rp

Väliranta, M., Korhola, A., Seppä, H., Tuittila, E.S., Sarmaja-Korjonen, K., Laine, J., Alm, J., 2007. High-resolution reconstruction of wetness dynamics in a southern boreal raised bog, Finland, during the late Holocene: A quantitative approach. Holocene 17, 1093–1107. https://doi.org/10.1177/0959683607082550

Väliranta, M., Oinonen, M., Seppä, H., Korkonen, S., Juutinen, S., Tuittila, E.-S., 2014. Unexpected Problems in AMS 14C Dating of Fen Peat. Radiocarbon 56, 95–108. https://doi.org/10.2458/56.16917

Väliranta, M., Salonen, J.S., Heikkilä, M., Amon, L., Helmens, K., Klimaschewski, A., Kuhry, P., Kultti, S., Poska, A., Shala, S., Veski, S., Birks, H.H., 2015. Plant macrofossil evidence for an early onset of the Holocene summer thermal maximum in northernmost Europe. Nat. Commun. 6, 1–8. https://doi.org/10.1038/ncomms7809

Van Bellen, S., Dallaire, P.L., Garneau, M., Bergeron, Y., 2011. Quantifying spatial and temporal Holocene carbon accumulation in ombrotrophic peatlands of the Eastmain region, Quebec, Canada. Global Biogeochem. Cycles 25, 1–15. https://doi.org/10.1029/2010GB003877

Waddington, J.M., Roulet, N.T., 2000. Carbon balance of a boreal patterned peatland. Glob. Chang. Biol. 6, 87–97. https://doi.org/https://doi.org/10.1046/j.1365-2486.2000.00283.x

Watson, E.J., Swindles, G.T., Lawson, I.T., Savov, I.P., 2015. Spatial variability of tephra and carbon accumulation in a Holocene peatland. Quat. Sci. Rev. 124, 248–264. https://doi.org/10.1016/j.quascirev.2015.07.025

812 Weckström, J., Seppä, H., Korhola, A., 2010. Climatic influence on peatland formation and lateral expansion in sub-
813 arctic Fennoscandia. Boreas 39, 761–769. https://doi.org/10.1111/j.1502-3885.2010.00168.x

814 Wilson, R., Anchukaitis, K., Briffa, K.R., Büntgen, U., Cook, E., D'Arrigo, R., Davi, N., Esper, J., Frank, D.,
815 Gunnarson, B., Hegerl, G., Helama, S., Klesse, S., Krusic, P.J., Linderholm, H.W., Myglan, V., Osborn, T.J.,
816 Rydval, M., Schneider, L., Schurer, A., Wiles, G., Zhang, P., Zorita, E., 2016. Last millennium northern
817 hemisphere summer temperatures from tree rings: Part I: The long term context. Quat. Sci. Rev. 134, 1–18.
818 https://doi.org/10.1016/j.quascirev.2015.12.005

819 Wu, J., Roulet, N.T., 2014. Climate change reduces the capacity of northern peatlands to absorb the atmospheric carbon
820 dioxide: The different responses of bogs and fens. Global Biogeochem. Cycles 27, 1005–1024.
821 https://doi.org/doi:10.1002/ 2014GB004845

822 Young, D.M., Baird, A.J., Charman, D.J., Evans, C.D., Gallego-Sala, A. V., Gill, P.J., Hughes, P.D.M., Morris, P.J.,
823 Swindles, G.T., 2019. Misinterpreting carbon accumulation rates in records from near-surface peat. Sci. Rep. 9.
824 https://doi.org/10.1038/s41598-019-53879-8

825 Yu, Z., 2011. Holocene carbon flux histories of the world's peatlands: Global carbon-cycle implications. Holocene 21,
826 761–774. https://doi.org/10.1177/0959683610386982

827 Yu, Z., Beilman, D.W., Jones, M.C., 2009. Sensitivity of Northern Peatland Carbon Dynamics to Holocene Climate
828 Change. Carbon Cycl. North. Peatlands 55–69. https://doi.org/10.1029/2008GM000822

829 Yu, Z., Loisel, J., Brosseau, D.P., Beilman, D.W., Hunt, S.J., 2010. Global peatland dynamics since the Last Glacial
830 Maximum. Geophys. Res. Lett. 37, 1–5. https://doi.org/10.1029/2010GL043584

831 Zhang, H., Gallego-Sala, A. V., Amesbury, M.J., Charman, D.J., Piilo, S.R., Väliranta, M.M., 2018a. Inconsistent
832 Response of Arctic Permafrost Peatland Carbon Accumulation to Warm Climate Phases. Global Biogeochem.
833 Cycles 1605–1620. https://doi.org/10.1029/2018GB005980

834 Zhang, H., Piilo, S.R., Amesbury, M.J., Charman, D.J., Gallego-Sala, A. V., Väliranta, M.M., 2018b. The role of
835 climate change in regulating Arctic permafrost peatland hydrological and vegetation change over the last
836 millennium. Quat. Sci. Rev. 182, 121–130. https://doi.org/10.1016/j.quascirev.2018.01.003

837 Zhang, H., Väliranta, M., Piilo, S., Amesbury, M.J., Aquino-López, M.A., Roland, T.P., Salminen-Paatero, S., Paatero,
838 J., Lohila, A., Tuittila, E., 2020. Decreased carbon accumulation feedback driven by climate-induced drying of
839 two southern boreal bogs over recent centuries. Glob. Chang. Biol. 1–14. https://doi.org/10.1111/gcb.15005

840